UNIVERSITÀ
DI PAVIA

Dipartimento di Biologia e Biotecnologie "Lazzaro Spallanzani"

Laurea Magistralis in Molecular Biology and Genetics

Integrated molecular analysis of immunoglobulin gene rearrangements, class usage and CD79b expression in human high-grade B cell lymphomas

Analisi molecolare integrata dei riarrangiamenti dei geni delle immunoglobuline, dell'utilizzo delle classi isotipiche e dell'espressione di CD79b nei linfomi a cellule B umani ad alto grado.

Supervisor:
Prof Federico forneris

Co-supervisor (s), if any:
Prof Stefano Casola

Experimental thesis by
Viveka Selvarasa

Academic Year 2024/2025

Abstract (Italian)

Il recettore delle cellule B (B-cell receptor, BCR) è un regolatore cruciale della sopravvivenza, selezione e differenziamento dei linfociti B. Ogni BCR è costituito da un tetramero di catene pesanti (H) e leggere (L) delle immunoglobuline (IG), associate alle subunità di segnalazione CD79A e CD79B. Oltre al suo ruolo fisiologico, i segnali trasmessi dal BCR rappresentano un importante driver del processo di trasformazione che conduce allo sviluppo dei linfomi a cellule B. I processi che rimodellano i loci delle IG, inclusi la ricombinazione V(D)J, l'ipermutazione somatica e lo switch isotipico di classe, generano diversità anticorpale e modulano la funzione effettrice delle IG stesse. Una regolazione aberrante di tali processi favorisce l'insorgenza di traslocazioni cromosomiche e mutazioni somatiche su scala genomica, conducendo alla trasformazione maligna. Sebbene la maggior parte dei linfomi a cellule B maturi conservi l'espressione del BCR, evidenze recenti del nostro laboratorio mettono in discussione questo paradigma, identificando una quota significativa di forme aggressive di linfoma a cellule B che silenziano l'espressione delle IG, precludendo la formazione di complessi BCR.

Lo scopo di questo studio è stato quello di indagare i meccanismi molecolari responsabili del silenziamento ricorrente dell'espressione delle IG in un sottotipo di linfoma potenzialmente letale rappresentato dai linfomi a cellule B ad alto grado con traslocazioni di *MYC* e *BCL2* (HGBCL-DH-*BCL2*). Per affrontare questo quesito, su campioni primari di HGBCL-DH-*BCL2* IGH-esprimenti e casi con IGH non rilevabile (IGH^{UND}), ho profilato e valutato la funzionalità dei riarrangiamenti dei geni variabili (V) delle IG, analizzato l'utilizzo delle classi isotipiche dell'IGH e studiato l'espressione della subunità responsabile di segnalare dal BCR, CD79B, al fine di stabilire se uno o più di questi determinanti possano essere responsabili e/o preferenzialmente associati al silenziamento del BCR in HGBCL-DH-*BCL2*.

Analisi molecolari sui campioni di linfoma hanno rivelato una marcata eterogeneità nell'utilizzo dei riarrangiamenti dei geni V delle catene IGH e IGL tra i casi IGH^{+} e IGH^{UND}. I tumori con BCR silenziato conservavano sistematicamente geni V dell'IGH potenzialmente produttivi, escludendo le mutazioni inattivanti come meccanismo generale responsabile del silenziamento dell'IGH a livello proteico. L'analisi dei riarrangiamenti dei geni V delle catene leggere ha mostrato un quadro più complesso, con identificazione ripetuta di riarrangiamenti non funzionali derivanti dalla stessa popolazione clonale di cellule B tumorali. L'analisi dell'utilizzo delle classi isotipiche dell'IGH ha evidenziato una chiara dicotomia tra tumori IGH-positivi e IGH^{UND}. I casi IGH^{+} erano frequentemente associati ad alterazioni strutturali della regione genomica switch-μ dell'IGH, con impatto negativo sul processo di IG CSR,

favorendo al contempo il mantenimento dell'espressione di IGM. Al contrario, i tumori IGH^{UND} completavano sistematicamente il processo di CSR, come indicato dalla perdita del gene *IGHM* e dall'espressione di trascritti per catene costanti IGH indicative di IG CSR (es IGG). Pertanto, mentre linfomi HGBCL-DH-*BCL2* IGH^{+} derivano principalmente da linfociti B che selezionano IGM come BCR, i corrispettivi IGH^{UND} originano da precursori linfomatosi che hanno completato IG CSR, sostituendo IGM con IGG o IGA. Infine, la quantificazione dei trascritti del gene *CD79B* ha evidenziato una marcata variabilità tra i diversi linfomi HGBCL-DH-*BCL2*, indipendentemente dallo stato IGH. L'analisi qualitativa di una variante di splicing di CD79B con skipping dell'esone 3, codificante per una proteina incapace di associarsi alla catena IGH, ha escluso una sua espressione preferenziale nei casi IGH^{UND}.

Questo studio ha studiato tre distinti meccanismi potenzialmente coinvolti nel silenziamento di IG/BCR nei linfomi HGBCL-DH-*BCL2*. I dati indicano che il silenziamento del BCR osservato nella maggior parte di questi tumori non è dovuto a mutazioni nonsense e/o frameshift che compromettano la funzionalità dei geni *IGHV*. L'analisi del repertorio dei geni V delle catene leggere nei casi IGH^{UND} ha evidenziato ripetutamente riarrangiamenti non produttivi, spesso associati all'espressione delle ricombinasi RAG1/2, suggerendo un processo riconducibile al cosiddetto receptor editing. Il silenziamento di espressione della proteina IGH nei linfomi HGBCL-DH-*BCL2* risulta principalmente associato all'espressione, da parte della cellula precursore del linfoma, di catene IGH che hanno completato il processo di switch isotipico di classe, mentre i tumori IGH^{+} conservano l'espressione di IGM. Questi risultati supportano un modello in cui l'isotipo IGH influenza la traiettoria evolutiva che determina lo sviluppo di linfomi HGBCL-DH-*BCL2* IGH^{+} e IGH^{UND}. Infine, i livelli di trascritti del gene *CD79B* risultavano altamente variabili sia nei casi IGH^{+} che in quelli IGH^{UND}, escludendo uno spegnimento del gene CD79B come causa principale del silenziamento del BCR. Analogamente, l'espressione di un'isoforma di mRNA di *CD79B* con skipping dell'esone 3, che impedisce l'associazione con la catena IGH, non risultava arricchita nei linfomi IGH^{UND}.

Nel complesso, questo lavoro ha contribuito a definire la relazione tra integrità dei geni V dell'IGH e IGL, classe isotipica dell'IGH e il silenziamento del complesso BCR nei linfomi HGBCL-DH-*BCL2*. Lo studio ha inoltre esplorato la possibilità che tale silenziamento sia causato da variazioni nell'espressione di CD79B e/o dalla selezione di specifiche isoforme di splicing. L'integrazione dei dati identifica il processo di "receptor editing" delle catene leggere delle immunoglobuline, nonche' la selezione di particolari classi isotipiche dell'IGH, come determinanti potenzialmente contribuenti al silenziamento del BCR nei linfomi HGBCL-DH-*BCL2*.

Abstract (English)

The B-cell receptor (BCR) is a central regulator of B cell survival, selection, and differentiation. Each BCR is expressed in multiple identical copies on the surface of a B lymphocyte and consists of a tetramer of immunoglobulin (IG) heavy (H) and light (L) chains associated with the signalling subunits CD79A and CD79B. Beyond its physiological role, BCR signalling is a key driver of B cell lymphomagenesis. Genetic processes targeting the IG loci, including V(D)J recombination, IG somatic hypermutation (SHM), and IG class switch recombination (CSR), generate antibody diversity and modulate IG effector function. Aberrant regulation of these processes favours the occurrence of chromosomal translocations, genome-wide somatic mutations, eventually leading to malignant transformation. While most mature B cell lymphomas preserve BCR expression, recent evidence challenges this paradigm by identifying a sizeable fraction of aggressive forms of B-cell lymphoma that silence IG expression precluding the formation of antigen receptor complexes.

The aim of this study was to investigate the molecular mechanisms responsible for the recurrent silencing of IG expression in a life-threatening lymphoma subtype represented by high-grade B-cell lymphomas with MYC and *BCL2* rearrangements (HGBCL-DH-*BCL2*). To address this question, I performed three sets of molecular analyses to investigate the expression and functional status of compoennets of the BCR in representative primary HGBCL-DH-*BCL2* tissue specimens, differentiating IGH-expressing from IGH-undetectable (IGH^{UND}) cases. Specifically, I profiled and assessed the functionality of IG variable (V) gene rearrangements, monitored IGH class usage, and analysed the expression of the BCR signalling subunit CD79B to establish whether any of these three determinants could be responsible for and/or preferentially associated with BCR silencing in a high proportion of HGBCL-DH-*BCL2*.

Comprehensive molecular analysis of lymphoma specimens revealed substantial heterogeneity in the usage of IGH and IGL chain V gene rearrangements across IGH^{+} and IGH^{UND} cases with no skewing in V gene usage. BCR-silenced tumors consistently retained potentially productive IGH V genes, excluding crippling mutations as a general mechanism responsible for IGH silencing observed at the protein level. IG light chain V gene profiling showed a more complex pattern with repeated identification of several non-functional rearrangements originating from the same clonal B cell population. Analysis of IGH class usage showed a clear dichotomy between IGH-positive and IGH^{UND} tumors. IGH^{+} HGBCL-DH-*BCL2* cases predominantly expressed IGM and were frequently associated with structural alterations of the IGH switch-μ region, precluding efficient IG CSR, while enforcing IGM expression. In contrast, IGH^{UND}

tumors consistently completed IG CSR, as indicated by the loss of the *IGHM* constant region gene and the preferential detection of IGH-switched transcripts. Therefore, whereas IGH^{+} HGBCL-DH-*BCL2* derive primarily from IGM-expressing B cells, IGH^{UND} counterparts arise from lymphoma precursors that had undergone IG CSR to become IGG- or IGA-expressing cells. Finally, quantitative CD79B transcript measurements revealed marked inter-lymphoma variability irrespective of IGH status. Qualitative analysis of an exon-3 skipped *CD79B* splice variant, coding for a protein unable to pair with the IGH chain, excluded its preferential expression in the IGH^{UND} subset of HGBCL-DH-*BCL2* cases.

This study has investigated three distinct mechanisms potentially contributing to IG/BCR silencing in HGBCL-DH-*BCL2*, a highly aggressive lymphoma subtype with limited therapeutic options. The data indicate that BCR silencing observed in most of these tumors, is not caused by nonsense and/or frameshift mutations interfering with functionality of IGH V genes. Analysis of the IG light chain V gene repertoire of IGH^{UND} HGBCL-DH-*BCl2* repeatedly revealed non-productive rearrangements, often associated to the expression of the RAG1/2 recombinases reminiscent of a process called receptor editing.

IGH silencing in HGBCL-DH-*BCL2* is primarily associated with the expression of isotype-switched IGH chains by the lymphoma precursor cell, while IGH^{+} tumors preferentially retain IGM expression. These results support a model in which antibody class influences the evolutionary trajectory leading respectively to IGH^{+} and IGH^{UND} HGBCL-DH-*BCL2*.

Finally, CD79B transcript levels were highly variable in both IGH^{+} and IGH^{UND} HGBCL-DH-*BCL2*, excluding *CD79B* mRNA downregulation as a major mechanistic determinant for BCR silencing in these tumors. Similarly, expression of an exon-3 skipped *CD79B* mRNA isoform preventing CD79B pairing to the IGH chain was not enriched among IGH^{UND} HGBCL-DH-*BCL2* cases.

Collectively, my work has contributed to establishing the relationship between IGH V gene integrity, isotype class choice, and BCR silencing in HGBCL-DH-*BCL2*. I have also explored the possibility that BCR silencing in these lymphomas is linked to changes in *CD79B* expression and/or isofom selection. Integration of the data identifies IG light chain receptor editing and IGH class selection as major determinants associated with, and potentially contributing to, BCR silencing in HGBCL-DH-*BCL2*.

Keywords

B cell receptor, lymphoma; V(D)J recombination; Immunoglobulin class switch recombination; CD79B.

Table of Contents

1. Introduction

1.1. The B Cell Receptor

The B cell receptor (BCR) is a defining feature of B lymphocytes and a central mediator of adaptive immunity. It consists of two membrane-bound IGH chains paired with two corresponding IGL chains both carrying a variable (V) region domain conferring unique antigen specificity. Each IGH/L chain tetramer is non-covalently associated with the signalling heterodimer CD79A (Igα) and CD79B (Igβ) (Tkachenko, Kupcova and Havranek, 2023). Each B cell expresses a unique BCR specificity generated through the process of V(D)J recombination. The complexity of the BCR primary repertoire is estimated to be over 10^{11} unique specificities in humans. This configuration enables the immune system to recognize an almost inexhaustible diversity of antigens, forming the molecular basis of humoral immunity. However, antigen-binding capacity alone does not fully explain the biological role of the BCR. IGs lack intrinsic signalling capacity and instead rely on their association with CD79A and

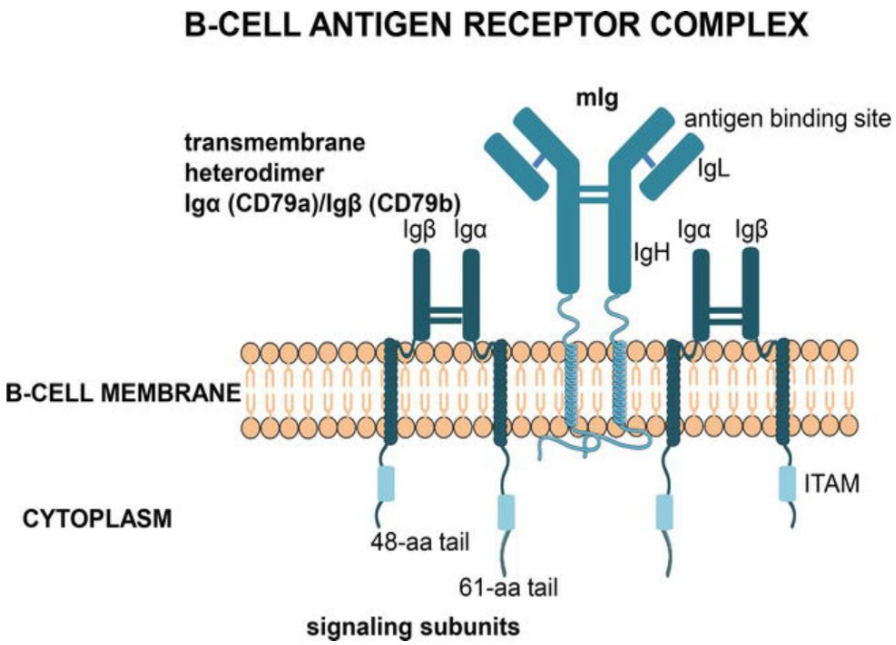

Figure 1: B-cell antigen receptor complex Source: (Aribi, 2020)

The B-cell antigen receptor (BCR) complex consists of membrane-bound IGH and IGL chains responsible for antigen binding, associated with the signalling subunits CD79A (Igα) and CD79b (Igβ). These subunits harbour cytoplasmic ITAM motifs that are critical for the initiation of intracellular signalling upon antigen engagement.

CD79B, which contain immunoreceptor tyrosine-based activation motifs (ITAMs) (Wen et al., 2019). These motifs are essential for initiating intracellular signalling following antigen engagement. Conformational changes in the receptor complex after antigen binding promote ITAM phosphorylation, permitting recruitment and activation of downstream kinases such as SYK (Liu et al., 2022). Through this physical coupling of antigen recognition and signal transduction, extracellular antigenic cues are efficiently converted into intracellular responses.

1.2. BCR signalling and functional outcomes in normal B Cells

Antigen binding triggers BCR signalling through initial receptor clustering and conformational changes that permit activation of Src-family kinases such as Lyn, followed by recruitment and activation of spleen tyrosine kinase (SYK) (Brian 4th and Freedman, 2021). This leads to phosphorylation of ITAM motifs and assembly of a signalling complex that propagates intracellular signals. Major downstream pathways include NF-κB, PI3K/AKT, and MAPK, each contributing to the regulation of B-cell survival, proliferation, differentiation, and metabolism (Balaji et al., 2018). Notably, BCR signalling is neither uniform nor strictly binary but highly dynamic and context dependent, with the strength, duration, and spatial organisation of signals ultimately determining cell fate. Weaker, tonic signalling supports anti-apoptotic pathways and basal survival, whereas stronger antigen-driven signals promote clonal expansion and differentiation into plasma cells or memory B cells. Excessive or prolonged BCR signalling can induce apoptosis, eliminating among others, autoreactive newly formed B cell clones. This graded signalling response is essential for maintaining immune homeostasis. Dysregulated BCR signalling has major consequences: insufficient signalling impairs B-cell survival and can lead to immunodeficiency, whereas excessive signalling promotes autoimmunity or contributes to malignant transformation (Preite et al., 2019). Signal thresholds are tightly controlled by co-receptors and regulatory molecules, including CD19, CD22, and FcγRIIB, which fine-tune BCR outputs (Chen et al., 2025). Additional complexity arises from crosstalk with other receptors, such as Toll-like receptors (TLRs) and cytokine receptors, allowing integration of antigen-specific and innate immune cues to shape B-cell responses. For instance, co-engagement of BCR and TLRs can amplify signalling and drive terminal differentiation to antibody secereting plasma cells, particularly during infection. Because BCR signalling orchestrates activation, tolerance, and apoptosis (Berry et al., 2020), even subtle

perturbations in these pathways can have lasting effects, and uncontrolled signalling is a key driver of autoimmune disease and B-cell malignancies.

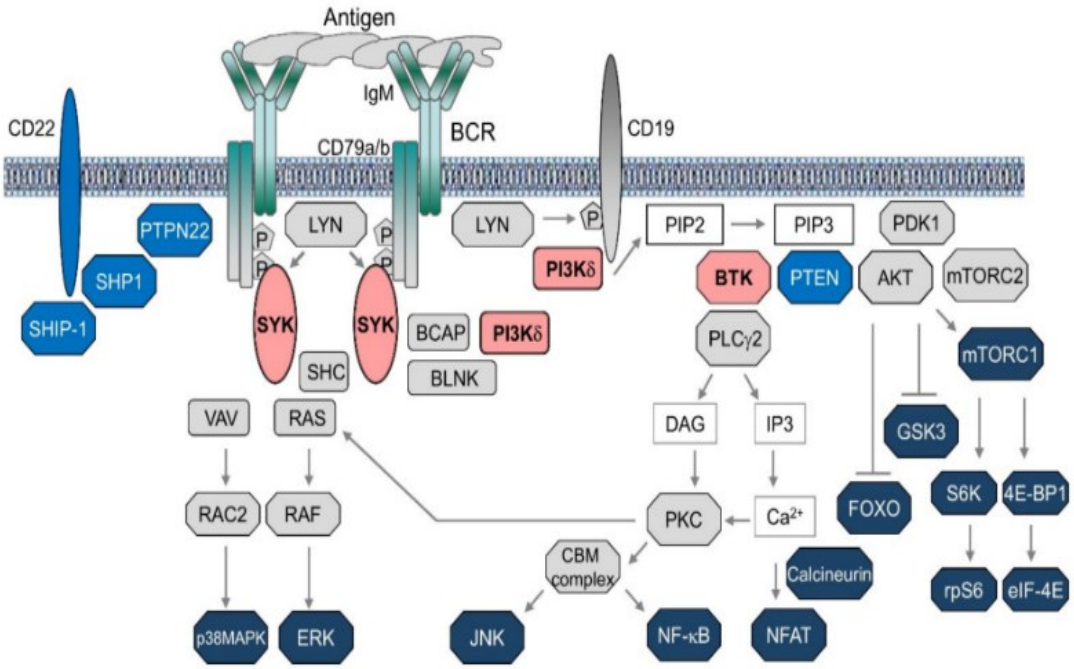

Figure 2: Overview of B-cell receptor signalling pathways Source: Efremov, Turkalj and Laurenti, 2020

Figure 2 illustrates BCR signalling pathways triggered by antigen engagement. Activation of CD79A/B recruits' kinases such as LYN and SYK, which in turn activate downstream cascades including PI3K, BTK, and PLCγ2. These pathways converge on NF-κB, MAPK, and AKT signalling, thereby regulating B-cell survival, proliferation, and differentiation, while co-receptors such as CD19 modulate signal strength. The combined activity of these pathways, rather than any single route, determines overall signalling output, but the precise mechanisms by which B cells establish and adjust these signalling thresholds remain incompletely defined.

1.3. The BCR control of early B cell development

B-cell development is a tightly regulated process that occurs in the bone marrow and generates a diverse self-tolerant B-cell repertoire. Haematopoietic stem cells progress through a series of stages, pro-B, pre-B, immature B, and mature naive B cells, each defined by characteristic molecular and phenotypic changes (Winkler and Mårtensson, 2018). A key feature of this developmental trajectory is the generation of BCR diversity through V(D)J recombination. The recombination-activating genes RAG1 and RAG2 initiate V(D)J recombination by introducing

site-specific double-strand breaks at recombination signal sequences. These breaks are repaired by non-homologous end joining DNA repair factors, generating a variable (V) region gene from the joining of individual variable (V), diversity (D), and joining (J) gene segments. As a result, the antigen receptors produced are highly diverse, enabling the immune system to recognize a wide range of pathogens. However, DNA double-strand breaks inherently pose a risk of genomic instability (Winkler and Mårtensson, 2018). Errors in the DNA repair process can lead to chromosomal translocations, making V(D)J recombination both essential for immune diversity and a potential source of genomic vulnerability. The first developmental checkpoint in B cell development is mediated by assembly of a pre-B cell receptor (pre-BCR). In pro-B cells expression of a functional pre-BCR relies on successful competion of a IGH chain V gene rearrangement and allows progression to the pre-B cell stage (Wong et al., 2019). In pre-B cells, RAG recombination targets the IGL chain chain loci, IG-kappa or IG-lambda, to catalyze VJ recombination. Productive IGL chain V gene rearrangements followed by successful pairing of IGH and IGL chains leads to the transit from the pre-B to the immature B cell stage strictly dependent on surface expression of a functional BCR.

Negative selection shapes the newly formed BCR repertoire by eliminating immature autoreactive cells, ensuring self-tolerance and preventing autoimmune disease. This process is not entirely efficient, and some autoreactive B cells escape into the periphery, where additional regulatory mechanisms are required to control them.

Overall, B-cell development reflects a balance between generating diversity and maintaining tolerance, a balance that is inherently imperfect and creates opportunities for pathogenic errors. This is particularly relevant in lymphoma, where aberrant V(D)J recombination events contributes to the outgrowth of B cell leukemias and lymphomas.

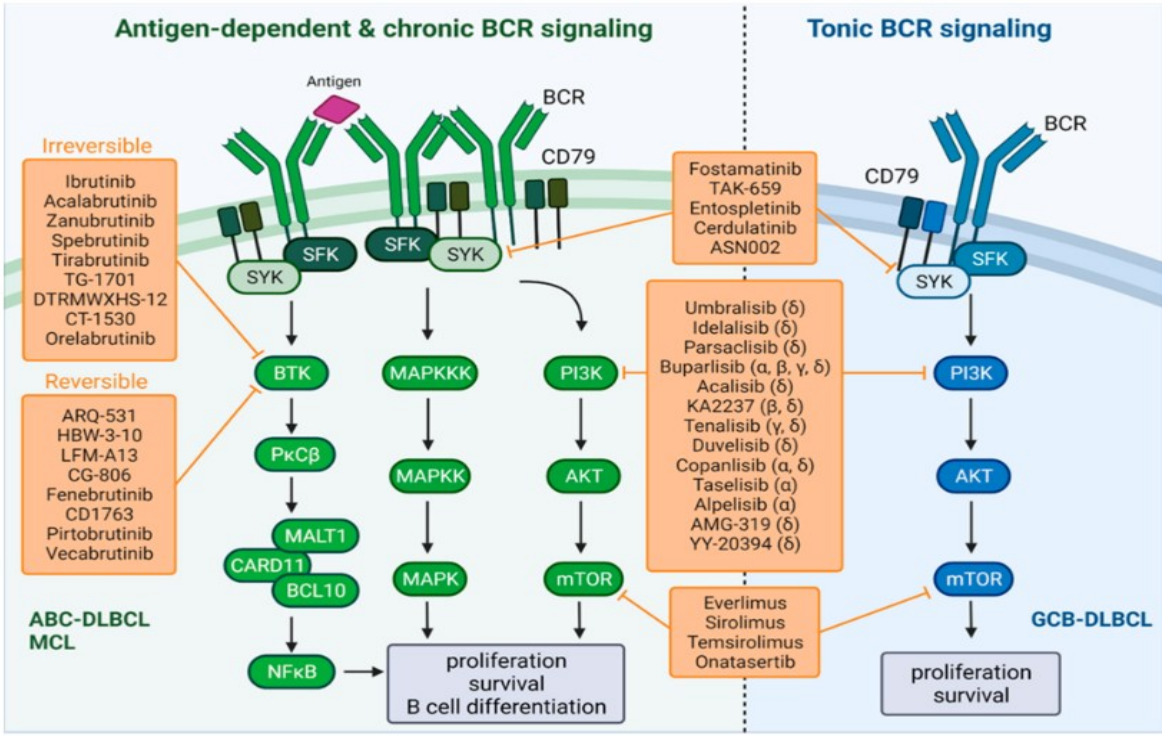

Figure 3: Regulation of BCR signalling and therapeutic inhibition of BTK and PI3K

Source: Profitos-Peleja et al., 2022

Figure 3 compares antigen-dependent chronic BCR signalling with tonic BCR signalling. Chronic signalling involves activation of SYK, BTK, MAPK, and PI3K, driving NF-κB-mediated proliferation and survival typical of ABC-DLBCL. In contrast, tonic signalling predominantly relies on PI3K-AKT-mTOR pathways to sustain survival in GCB-DLBCL. The figure also highlights therapeutic inhibitors targeting key components of these signalling cascades.

1.4. The BCR control of B cell immune responses: the key role played by the germinal center reaction

After antigen encounter through the BCR, activated B cells migrate to germinal centres (GC), specialized microenvironments in secondary lymphoid organs such as the spleen and lymph nodes (Rastogi et al., 2022). GCs consists of two spatially resolved zones where B cells exert distinct functions. In the GC dark zone (DZ), B cells undergo rapid proliferation while accumulating mutations into IG Varable region genes through the process called IG somatic hypermutation (SHM). IG SHM is initiated by the action of the activation-induced cytidine deaminase (AID) enzyme, which deaminates cytidines into IGV genes converting them into uracils which are in turn replaced through distinct DNA repair pathways including missmatch

repair and base excision repair, followed by the action of error-prone DNA polymerases. As a result of IG SHM, clonally related B cells acquire a distinct set of randomic single-nucleotide substitutions impacting on the original binding affinity of the BCR. After completion of a round of IG SHM, GC DZ B cells migrate to the GC light zone (LZ) area. Here B cells equipped with mutated BCRs compete with each other for the ability to capture antigen presented on the surface of follicular dendritic cells in the form of antigne-antibody immune complexes. Cells capturing more proteinaceous antigen thanks to improved BCR affinity, will intenalize and process more of it allowing a more efficient presentation of resulting peptides on MHC-class II complexes, to T-follicular helper (Tfh) cells (Martinez-Riano et al., 2023). Cells expressing

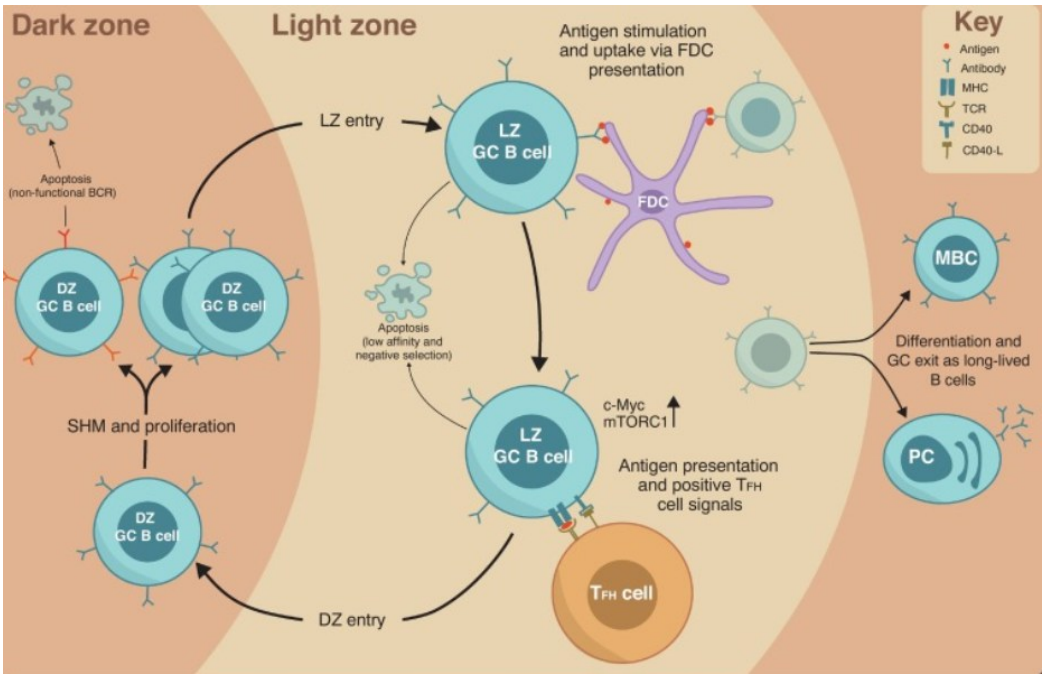

Figure 4: B-cell migration, interaction, and differentiation dynamics in the germinal centre Source: Gracie et al., 2025

Figure 4 depicts the germinal centre reaction, highlighting the coordination between dark and light zone processes. In the dark zone, B cells proliferate and acquire somatic hypermutations, whereas in the light zone they interact with follicular dendritic cells and Tfh cells for affinity-based selection. High-affinity clones survive and differentiate into memory B cells or plasma cells, while low-affinity cells are eliminated by apoptosis. Importantly, the germinal centre is also a major site of genomic instability: somatic hypermutation and class switch recombination generate DNA damage that must be repaired, creating opportunities for mutations and chromosomal translocations (Pilzecker and Jacobs, 2019).

high-affinity BCRs are therefore preferentially selected to survive, either re-entering into a further round of proliferation and IG SHM in the DZ area or exit the GC as antibody-secreting plasma cells, which represent terimally differentiated B cells, or as long-lived memory B cells which retain a high-affinity BCR on the surface. Memory B cells are preferentially recruited into secondary immune responses following repeated encounter of the host with the same foreign antigen. Memory B cells can either partecipate again in the GC reaction, or teerminally differentiate in antibody-screting plasma cells.
The process of antibody affinity maturation occuring in GCs as a result of iterative rounds of clonal expansion, IG SHM and antigen-driven selection remains at each stage strictly dependent on the expression of functional BCR complex (Ondrisova and Mraz, 2020).

Another major genetic rearrangement occuring in GC B cells is associated with the propoerty of B cells to switch the effector function of their BCRs. Whereas the dominant IGH chain class expressed by newly formed and later matured pre-GC B cells is represented by IGM, once B cells get recruited into the GC reaction, they often undergo the process called IG class switch recombination (CSR). IG CSR allows a B cells to replace the IGM constant region with that of another class including in humans IGG1, IGG2, IGG3, IGG4 IGA1 and IGA2. The replacement of IGM with that of another IGH class leads to major qualitative and quantitative changes in BCR signaling, as well as to the capacity to more effectively activate other arms of the immune system, including activation of the complement pathway, which preferentially binds to IGG antibodies as compared to their IGM counterparts. Binding of soluble IGG to the surface of pathogens favors local activation of the complement pathway ultimatly leading to the killing of the pathogen. As IG SHM, also IG CSR is iniated by AID which favors staggered DNA double-stranded breaks in specific genomic regions in the IGH chain locus called IG switch regions. Theese regions map proximal to each IGH constant region gene (i.e. IGG1, IGG2, IGG3 IGA1). During IG CSR, breaks introduced by AID in the IGH switch region preceding the *IGHM* constant region gene (also called *switch-mu*) concurr with similar breaks in one of the downstream IGH switch regions flanking the IGG or IGA constant region genes. Upon completion of IG CSR, the IgM constant region gene is deleted from the locus and rplaced by a downstream IGH constant region gene which is placed proximal to the functional IGHV gene ensuring expression of a full-length isotype-switched IGH transcript.

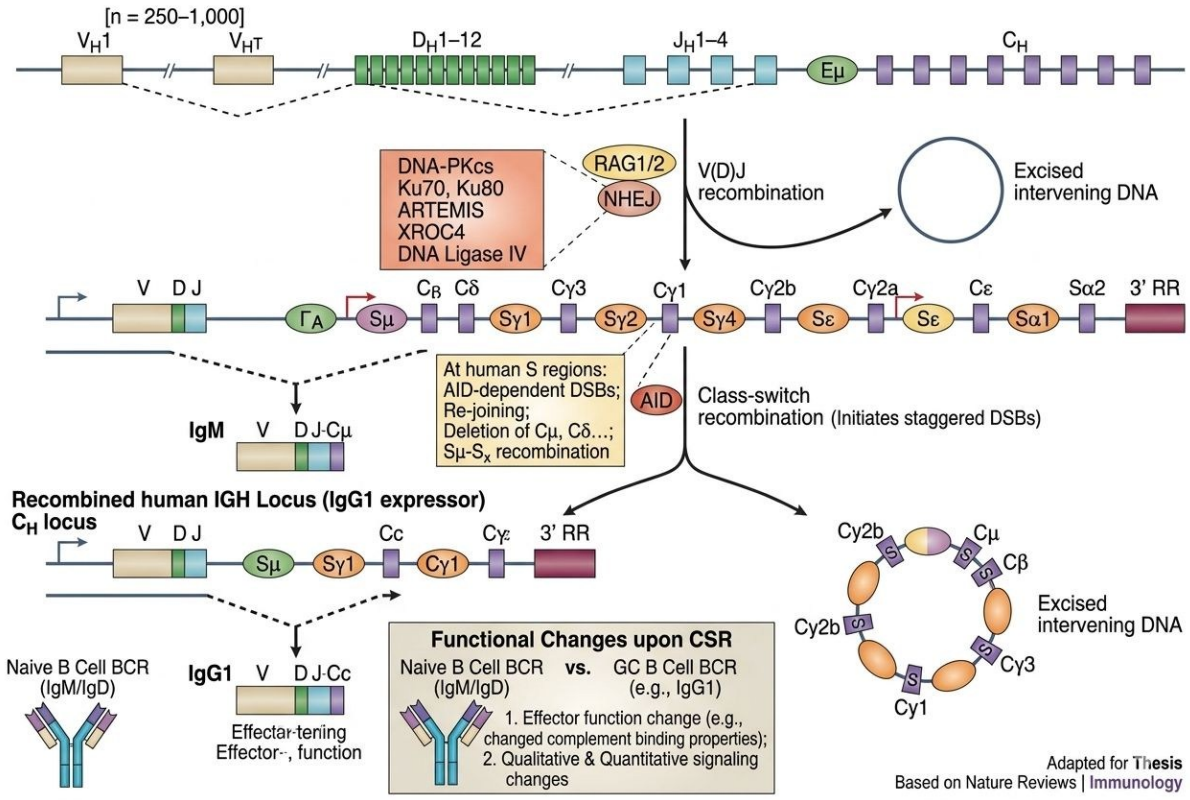

Figure 5: Mechanism of IGH Class Switch Recombination (CSR).

Source: Chaudhuri, J. & Alt, F. W. (2004)

The IGH locus contains the V(D)J region and downstream constant region genes (Cμ, Cγ, Cα, etc.), each preceded by switch (S) regions. Activation-induced cytidine deaminase (AID) introduces double-strand breaks in Sμ and a downstream S region corresponding to the target isotype. DNA repair deletes the intervening segment, positioning the selected constant region next to the V(D)J exon. This generates a full-length isotype-switched IGH transcript (e.g., IgG or IgA), replacing IgM, and modifies BCR signaling and effector functions. The excised DNA forms a circular episome

1.5. The B Cell Receptor and Lymphomas

1.5.1. The role of Immunoglobulin genetics in B cell lymphomagenesis

The BCR plays a central role in the pathogenesis of mature B-cell malignancies. The contribution of BCR biology to malignant B cell transformation starts with the genetic rearrangements responsible of the V(D)J recombination, IG SHM and IG CSR occuring respectively during early B cell development, and later upon partecipation of antigen-specific B cells in the GC reaction.

Aberrant V(D)J recombination cataglyzed by the *Rag1/2* genes is responsible of chromosomal translocations such as the t(14;18) placing the BCL2 oncogene in close proximity to *IGH* cis regulatory regions, ultimately causing deregulated constitutive expression of the oncoprotein. The t(14;18) translocation is the hallmark of Follicular Lymphoma (FL) a mature B cell lymphoma arising from BCL-2 rearranged B cells acquiring through the transit in the GC additional somatic mutations ultimately promoting the outgrowth of a milagnant clonal B cell neoplasm. Aberrant V(D)J recombination also cause the t(11:14) *IGH*::*CCND*1 chromosomal rearrangement driving constitutive expression of the cyclin gene and ultimately the outgrowth of rapidly proliferating mantle cell lymphoma.

IG light chain loci can also represent targets of aberrant VJ recombination. In particular, our lab has recently described the partecipation of the RAG1/2 recombination machinery to the generation of *IGL*::*MYC*, t(8;22) translocations responsible of the outgrowth of High-grade B cell lymphomas with MYC and BCL2 rearrangements (HGBCL-DH-BCl2)

Aberrant IGH CSR catalyzed by AID is instead the primary responsible of the t(8;14) chromosomal translocation responsible of Burkitt Lymphoma (BL), a GC B cell tumor characterized by the juxtaposition of the c-MYC gene to *IGH* cis regulatory regions, leading to deregulated expression of the oncoprotein.

Aberrant IG SHM is instead recurrently implicated in the introduction of single nucleotide substitutions and/or samll insertions/deletions in lymphoma relevant genes including *BCL6, BCL2, PAX5, BACH2, IRF4, MYC, CIITA and TCF4*.

Collectively these observations highlight the relevance of immunoglobulin genetics in the origin of B cell lymphomas, representing the dark side of B cell immunity.

1.5.2. The role of BCR signaling in B cell lymphomagenesis

Malignant B cells frequently hijack the same pathways that support normal B-cell survival and proliferation (Burger and Wiestner, 2018). Two principal forms of oncogenic B-cell receptor (BCR) signalling have been described: chronic active signalling and tonic signalling.

Chronic active BCR signalling arises in a permissive microenvironment for malignant transformation and typically depends on engagement with self-antigens or environmental antigens (Bagnara et al., 2022). It is exemplified by activated B cell–like diffuse large B-cell lymphoma (ABC-DLBCL), in which BCR-driven constitutive NF-κB activation promotes cell survival and proliferation. By contrast, tonic BCR signalling is antigen-independent and relies on low-level, constitutive PI3K-mediated signalling, as observed in BL (Gehringer et al., 2020).

These two signalling modes differ not only conceptually but also in their biological and therapeutic implications. Chronic active signalling, being persistent and often antigen-driven, is frequently associated with mutations in components of the BCR and Toll-like receptor (TLR) signalling pathways, such as CD79B or MYD88, which further amplify pathway activation. Tonic signalling, on the other hand, appears to be more dependent on BCR expression levels and basal signalling thresholds than on specific oncogenic mutations.

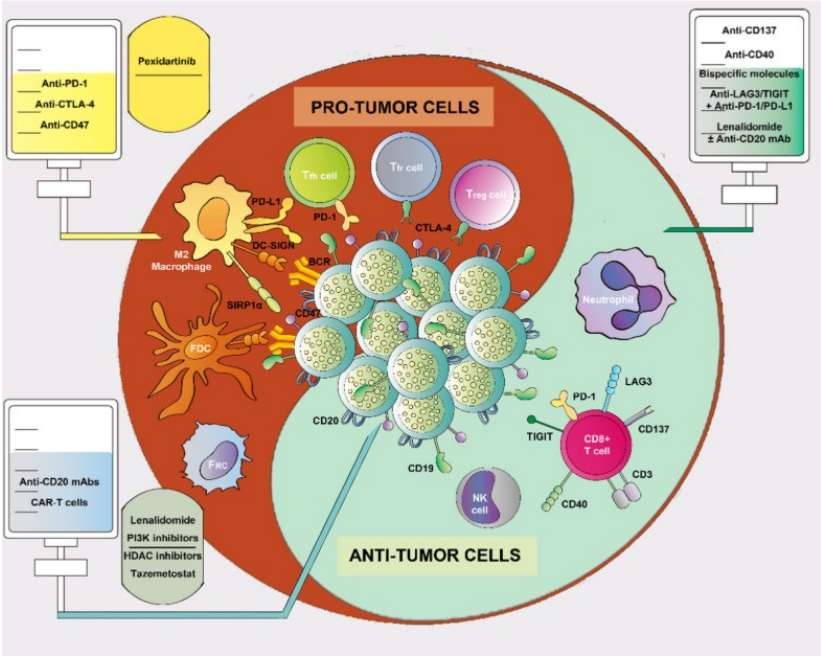

Figure 6: Roadmap of drugs directed against follicular lymphoma (FL)

Source: Blanco et al., 2022

Figure 6 depicts the lymphoma tumour microenvironment, where pro-tumour and anti-tumour immune cells interact. Malignant B cells engage immune checkpoints such as PD-1 and CTLA-4 to suppress T-cell activity, while macrophages, dendritic cells, and regulatory T cells provide additional tumour support. Therapeutic strategies targeting these pathways aim to enhance antitumour immunity and disrupt tumour-promoting cellular interactions.

A key unresolved question is whether all B-cell lymphomas share the same degree of dependence on BCR signalling. While many entities exhibit clear BCR addiction, others can downregulate or even lose BCR expression altogether. This suggests that BCR dependency varies across lymphoma subtypes and disease stages. Such variability has important therapeutic implications, as tumours lacking functional BCR signalling are unlikely to respond to BCR pathway inhibitors. Thus, although BCR signalling is a well-established driver of

lymphomagenesis, its contribution is highly context-dependent and heterogeneous across tumours. A detailed understanding of how BCR expression and signalling are regulated in different lymphoma settings is therefore crucial for both biological interpretation and clinical application.

1.5.3. BCR expression and class varies across mature B cell neoplasms

B-cell neoplasms arising from mature B cells have long been thought to retain surface expression of the B-cell receptor (BCR) on malignant cells. This paradigm applies to tumors originating from pre–germinal center (pre-GC) B cells, such as chronic lymphocytic leukemia and mantle cell lymphoma, as well as to malignancies derived from germinal center (GC)-experienced B cells, including diffuse large B-cell lymphoma (DLBCL), Burkitt lymphoma (BL), and follicular lymphoma (FL). However, recent work, including studies from our laboratory, has challenged this assumption.

Through a comprehensive immunohistochemical analysis of class-specific IGH proteins (IGM, IGG, IGA) in primary lymphoma samples classified as BL, DLBCL, and HGBCL-DH-*BCL2*, a particularly aggressive subtype characterized by MYC and BCL2 rearrangements, we observed marked heterogeneity in immunoglobulin expression. While the majority of tumors retained IG expression, a substantial fraction displayed partial or complete silencing of IGH protein across the malignant population. Notably, uniform BCR silencing was predominantly observed in GC-derived HGBCL-DH-*BCL2*, in which more than two-thirds of cases were classified as IGH-undetectable (IGH^{UND}) by immunohistochemistry (our data; Hilton et al., *Blood*, 2024).

These findings were further substantiated by biochemical analyses showing that IGH^{UND} HGBCL-DH-*BCL2* fail to assemble functional BCR complexes, as evidenced by the absence of detectable interactions between IGH and CD79A or CD79B. This supports the notion that loss of IGH expression results in structural disruption of the receptor complex. Importantly, our studies also revealed a link between BCR expression status and IGH isotype selection in the lymphoma precursor cells. Whereas IGH-positive HGBCL-DH-*BCL2* predominantly express unswitched IGM, IGH^{UND} cases consistently originate from class-switched (IGG or IGA) GC B cells.

Collectively, these findings reveal a far more complex landscape than previously appreciated, in which variability in BCR expression and IGH class delineates biologically distinct lymphoma subsets within the same histological and genetic categories. In particular, the observation that mature GC B cells can give rise to lymphomas that have extinguished BCR

expression has important mechanistic and clinical implications. It raises fundamental questions about how malignant B cells bypass dependence on BCR signalling and has direct therapeutic relevance, given the increasing use of antibody–drug conjugates targeting CD79B, which rely on surface BCR expression for effective tumor cell targeting.

1.5.4. The BCR Signalling subunits CD79A and CD79B in mature B cell neoplasms

CD79A and CD79B are integral components of the B-cell receptor (BCR) complex and act as the primary mediators of intracellular signal transduction following antigen engagement (Tkachenko, Kupcova and Havranek, 2023). These transmembrane proteins contain immunoreceptor tyrosine-based activation motifs (ITAMs) in their cytoplasmic domains, which are phosphorylated by Src family kinases upon BCR activation. ITAM phosphorylation enables recruitment of spleen tyrosine kinase (SYK) and the assembly of downstream signalling complexes, ultimately leading to activation of NF-κB, PI3K/AKT, and MAPK pathways. CD79A and CD79B therefore function not merely as accessory molecules, but as essential transducers that couple antigen recognition to cellular responses. In their absence, the immunoglobulin component of the BCR is signalling-incompetent, underscoring the interdependence between structural integrity and signalling competence of the receptor complex (Seon et al., 2024).

In diffuse large B-cell lymphoma (DLBCL), particularly in the activated B cell–like (ABC-DLBCL) subtype, gain-of-function mutations in CD79B are common and are associated with increased surface BCR expression and chronic active signalling (Young et al., 2019). Mechanistically, these mutations often impair receptor internalisation, thereby prolonging signal duration and sustaining NF-κB activation. This exemplifies how alterations in CD79A/B can enhance oncogenic BCR signalling.

Conversely, we have recently linked reduced expression of CD79B protein to the IGH^{UND} phenotype of HGBCL-DH-*BCL2*, pointing to a tight regulatory relationship between the immunoglobulin heavy chain (IGH) and CD79B. This coupling is likely inherited from precursor cells. For instance, germinal center dark zone (GC-DZ) B cells undergo marked downregulation of surface BCR, accompanied by reduced CD79B protein levels. This physiological state is recapitulated in IGH^{UND} HGBCL-DH-*BCL2*, consistent with their derivation from GC-DZ B cells.

CD79B has recently emerged as a major therapeutic target in frontline treatment of aggressive B-cell lymphomas, including DLBCL and HGBCL. The antibody-drug conjugate polatuzumab vedotin (Pola-V) binds surface CD79B in the context of the BCR and exploits receptor internalisation to deliver a cytotoxic payload, monomethyl auristatin E (MMAE), into malignant B cells. MMAE disrupts microtubule polymerisation, thereby blocking mitosis and inducing rapid cell death.

The identification of IGH^{UND} mature B-cell lymphomas poses a significant challenge for Pola-V-based therapies, as the target antigen is absent from the cell surface. This mechanism may explain observations from multiple clinical studies reporting reduced efficacy of Pola-V-containing regimens in patients with germinal center B cell-like (GCB) DLBCL and HGBCL-DH-*BCL2*, both of which frequently exhibit silencing of surface BCR expression.

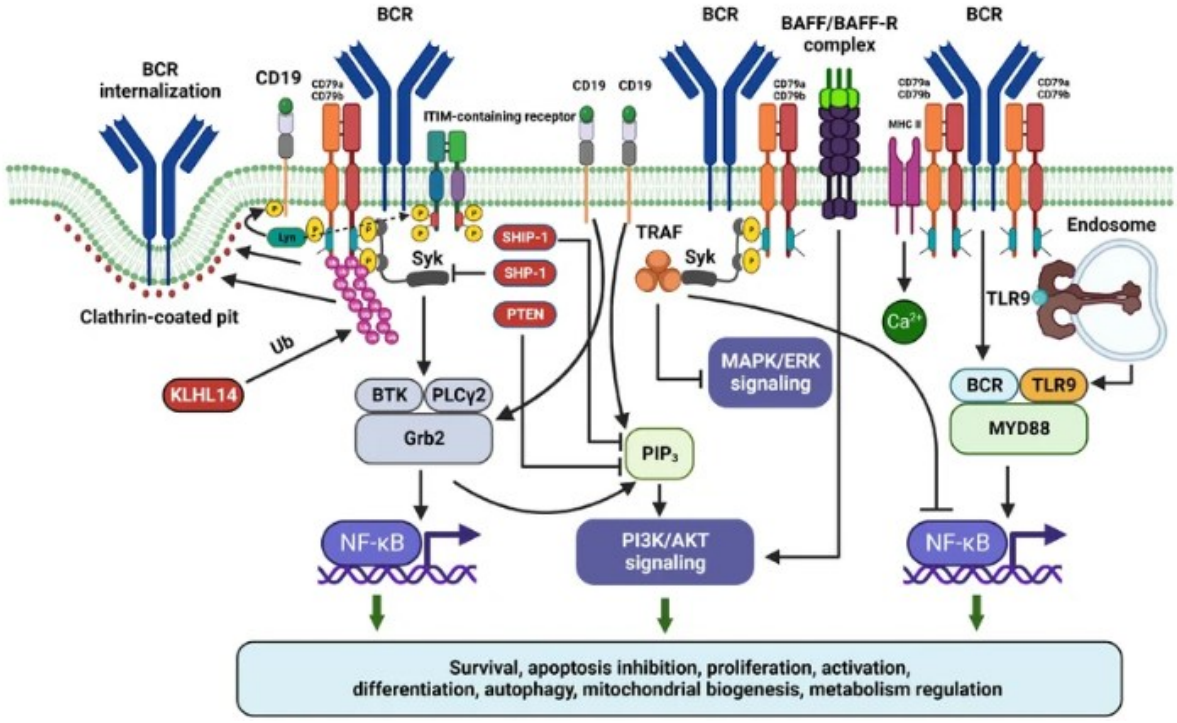

Figure 7: Role of CD79a/CD79b in B-cell receptor signalling in normal B cells

Source: Tkachenko, Kupcova and Havranek, 2023

Figure 7 outlines BCR signalling and its regulation, including receptor internalisation and interactions with co-receptors such as CD19 and BAFF-R. Activation of kinases including SYK, BTK, and PLCγ2 initiates PI3K/AKT, MAPK/ERK, and NF-κB pathways, which together regulate B-cell survival, proliferation, differentiation, and metabolism. Crosstalk with TLR9 further modulates these responses. Regulation of CD79A/B expression and function can

reflect broader changes in transcriptional control, protein stability, or local signalling organisation. Consequently, analysing CD79a/b provides a useful framework for distinguishing structural defects in BCR assembly from alterations in signalling capacity. These distinctions are essential for understanding heterogeneity in BCR dependency among lymphomas and for predicting responses to BCR-targeted therapies.

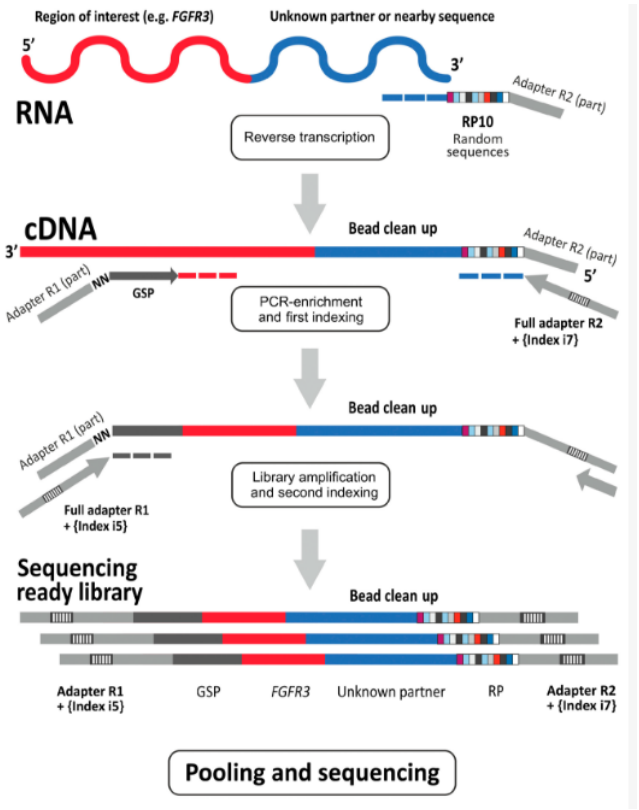

Figure 8: NGS library preparation using a 3′ RACE-based method

Source: Mitiushkina et al., 2024

2. Aim of the work

The recent identification of IGH^{UND} subsets of HGBCL-DH-*BCL2* challenges the long-standing paradigm that mature B-cell lymphomas universally retain a functional BCR. These findings raise fundamental mechanistic questions regarding how malignant B cells can bypass dependence on BCR signalling, and what molecular events underlie the loss of receptor expression.

Building on these observations, the work presented in this thesis is aimed at dissecting the molecular basis of BCR silencing in HGBCL-DH-*BCL2*, with a focus on three main objectives.

First, to determine whether structural alterations of the immunoglobulin genes contribute to BCR loss, I reconstructed full-length IGH and immunoglobulin light chain variable (V) region sequences from BCR-silenced HGBCL-DH-*BCL2* cases using 5′ rapid amplification of cDNA ends (5′ RACE). This approach enabled the assessment of V(D)J recombination integrity and the identification of potential abnormalities affecting productive IG expression.

Second, to investigate the relationship between BCR expression and IGH class selection, I performed IGH class-specific RT-PCR analyses to define the isotype usage in IGH-positive and IGH^{UND} HGBCL-DH-*BCL2* cases. This analysis was further extended to explore the mechanisms underlying the apparent failure of IGM^{+} cases to complete CSR toward downstream IGh classes, providing insights into the genetic basis of this phenomenon.

Third, given the central role of CD79B in BCR assembly and signalling, I examined CD79B expression in representative HGBCL-DH-*BCL2* cases stratified by IGH status. This analysis included both quantitative assessment of CD79B transcript levels and isoform-specific characterization of CD79B mRNA to determine whether altered expression and/or alternative splicing contribute to the reduced CD79B protein levels observed in IGH^{UND} lymphomas.

Collectively, these approaches aim to provide a mechanistic framework linking IG gene configuration, class-switching status, and CD79B regulation to the loss of BCR expression in aggressive B-cell lymphomas. By integrating these molecular insights with the phenotypic characterization described above, this study seeks to elucidate how BCR silencing is established and maintained, and to define its biological and therapeutic implications.

All research activities described in the thesis were conducted at the AIRC Institute of Molecular Oncology, IFOM-ETS, Milan, under the supervision of Prof Stefano Casola (Principal Investigator leading the Genetics of B Cells and Lymphomas Laboratory at IFOM-ETS, and Associate Professor of General Pathology, Department of Medical Biotechnology and Translational Medicine, University of Milan, Italy).

3. Materials and Methods

3.1. Human participants

Experimental procedures involving human biological samples were conducted in strict adherence to the ethical standards of the institutional research committees of clinical centers that were involved in the study (ASST Spedali Civili, Brescia, Fondazione IRCCS Ca' Granda Ospedale Maggiore Policlinico, Milano). All procedures were performed in accordance with the Declaration of Helsinki. Prior to enrolment, written informed consent was obtained from all participants. The study cohort comprised n = 32 patients diagnosed with High-Grade B-Cell Lymphoma with rearrangements of *MYC* and *BCL2* (HGBCL-DH-*BCL2*). Primary tumor samples were obtained via surgical biopsy, immediately snap-frozen in liquid nitrogen, and stored at -80°C to preserve the integrity of nucleic acids and protein structures until further processing.

3.2. HGBCL-DH-*BCL2(-BCL6)* and DLBCL cell lines

Diffuse Large B-Cell Lymphoma (DLBCL) cell lines, including OCI-LY7, WSU-DLBCL2, and SU-DHL-4 were purchased from DMSZ repository (German Collection of Microorganisms and Cell Cultures) and cultured in RPMI-1640 medium (Euroclone) supplemented with 10% heat-inactivated Fetal Bovine Serum (FBS) (Sigma-Aldrich), 2 mmol/L L-glutamine, 50 μmol/L β-mercaptoethanol, according to manufacturer's instructions. COH-DHL1 and COH-THL1 HGBC-DH-*BCL2*(-*BCL6*) patient derived cell lines were kindly provided by dr Joo Y. Song and Prof Wing C. Chan and cultured in RPMI-1640 medium (Euroclone) supplemented with 10% heat-inactivated FBS (Sigma-Aldrich), 2 mmol/L L-glutamine, supplemented with 10mmol/L HEPES (Euroclone) to maintain pH stability. All cells were cultured at a density of 0.5 - 1.5 × 10^6 cells/mL, at 37°C in a humidified atmosphere, with 5% CO2. To ensure experimental reproducibility, cell lines were periodically tested for Mycoplasma (MycoAlert Mycoplasma Detection Kit, Lonza). Cell line authentication was performed via short-tandem-repeat (STR) profiling using the GenePrint 10 System (10-Locus STR System for Cell Line Authentication, Promega).

3.3. Nucleic acid extraction

AllPrep DNA/RNA Mini Kit (Qiagen) was used for concomitant DNA and RNA extraction from human lymphoma cell lines or frozen tissue biopsies. Cultured cells (up to 5x106) were harvested by centrifugation at 300 x g for 5 minutes, washed once with ice-cold PBS, and lysed directly in RLT Plus buffer. The addition of β-mercaptoethanol was critical for effective lysis of these high-protein-content lymphoid cells. Frozen biopsies were subjected to mechanical

disruption using the TissueLyser II (Qiagen). Approximately 20 - 30 mg of frozen tissue was placed in a 2 mL microcentrifuge tube containing a 3 - 7 mm stainless steel beads and 600 µL of RLT Plus lysis buffer (supplemented with 1% β-mercaptoethanol to irreversibly denature RNases). To achieve complete homogenization, two consecutive cycles of 20 seconds at 30 Hz were performed. Between cycles, samples were kept on ice to prevent thermal degradation of RNA. Lysates obtained from cultured cell lines or homogenized frozen biopsies were passed through AllPrep DNA spin columns to allow binding of genomic DNA, while the flow-through was used for RNA purification via RNeasy spin column (Qiagen). DNA/RNA concentration and integrity were assessed using Qubit dsDNA HS Assay Kit (Thermo Fisher Scientific), NanoDrop 2000/2000c spectrophotometers, and Agilent 2100 Bioanalyzer system.

3.4. 5′ Rapid amplification of cDNA ends (5'RACE)

The 5'RACE protocol was adapted from Vazquez Bernat and colleagues (Vázquez Bernat et al., 2019). Briefly, total RNA was extracted using AllPrep DNA/RNA Mini Kit (QIAGEN), and first-strand cDNA synthesis reaction was performed using 200 ng of total RNA with 10 µmol/L oligo dT and Superscript II Reverse Transcriptase (Thermo Fisher Scientific) at 42°C for 1 hour. Template switching was carried out at 42°C for 1 hour by adding to the reaction mix a template switch oligonucleotide (Read1_TS, Table 3) composed of a five-nucleotide poly-guanosine (poly-G) stretch, a 12-nucleotide unique molecular identified, and an Illumina's universal amplification sequence (Read1). Following template switching, cDNA was purified using the Wizard SV Gel and PCR clean-up kit (Promega) according to the manufacturer's recommendation. 2X KAPA HiFi Hot Start Ready Mix (Roche) was used to amplify the purified cDNA template through a 2-step semi-nested PCR using forward Read1-specific primers (Read1-U) and two sets of class-specific IGH and lGK/L constant region gene-specific reverse primers (with second-round internal primers, including also the Illumina Read2 sequence). Primer sequences are listed in Table 3. A purification step was conducted after each PCR round using AMPure XP Bead-Based Reagent (Beckman Coulter Life Sciences) according to the manufacturer's instructions using a 0.65X beads-to-sample ratio, to selectively remove primer dimers while retaining the desired ~ 450 bp fragments. 10 ng of purified PCR products were indexed using 2X KAPA HiFi Hot Start Ready Mix, with forward (P5_R1) and reverse (P7_R2) indexing primers, in a 13-cycle index PCR reaction. Indexed libraries were purified using AMPure XP Beads, quality controlled using Agilent 2100 Bioanalyzer system, and sequenced (2 x 250 bp read length) on a MiSeq Illumina sequencer using MiSeq Reagent Kit v2, 300-cycles (Illumina).

3.5. Bioinformatic pipeline and clonotype identification

Raw paired-end FASTQ files were first merged using usearch (v.11.0.667) using standard parameters (90% identity, minimum merge length of 15 bp). Cutadapt (v.3.4) was used to recognize and trim 3' primers; any read lacking these primers was discarded to ensure high-quality data. To streamline the dataset and remove potential sequencing errors, sequences were "collapsed" (deduplicated) using a custom Python package, and sequences appearing only once were removed from the analysis. Functional annotation of the immunoglobulin segments (V, D, and J genes) was performed by aligning the processed sequences against the IMGT reference database using IgBlast (v.1.21.0). Sequences with identical CDR3 lengths and D-J gene assignments were grouped and subjected to agglomerative clustering to cluster the same clonotype sequences. This clustering used a dynamic distance cutoff tailored to the specific length of the CDR3 region, allowing for the precise grouping of sequences into distinct, biologically relevant clonotypes.

3.6. Detection of IGH switched vs unswitched sterile transcripts

Total RNA was extracted from human ymphoma cell lines using RNeasy Mini Extraction Kit (Qiagen) as described in section 3.3. Total RNA was reverse transcribed into complementary DNA (cDNA) using Superscript-III Reverse Transcriptase (Thermo Fisher Scientific) according to the manufacturer's recommendations. Briefly. 0.5–1 µg of total RNA was combined with 10 µmol/L oligo(dT) and 10 mM dNTP mix in nuclease-free water to a final volume of 10 µL, incubated at 65 °C for 5 min to denature secondary structures, and immediately chilled on ice. Reverse transcription was performed by adding 10 µL of a reaction mix containing 2 µL 10× RT buffer, 4 µL 25 mM $MgCl_2$, 2 µL 0.1 M DTT, 1 µL RNaseOUT recombinant RNase inhibitor, and 1 µL SuperScript III Reverse Transcriptase (200 U/µL). The reaction was incubated at 25 °C for 10 min to allow primer annealing, followed by cDNA synthesis at 50 °C for 50 min. The enzyme was inactivated by heating at 85 °C for 5 min, and residual RNA was removed by treatment with RNaseH (1 U, 20 min at 37 °C). Resulting cDNA was diluted 1:5 - 1:10 in nuclease-free water and used as template for downstream PCR analysis. To amplify transcripts initiated from the Iµ sterile exon located upstream of the IGHM constant region and spliced to downstream constant region genes following CSR, PCR reactions were designed using a forward primer annealing to the Iµ sterile exon and reverse primers annealing to the IGHG1 constant region. Primer sequences are indicated in table 3. PCR reactions were carried out in 25 µL volumes containing 1 - 2 µL of cDNA template, 0.2 µM of each primer, 200 µM dNTPs, 1X GoTaq Flexi buffer containing 2.5 mM $MgCl_2$, and 1

U thermostable GoTaq Flexi DNA polymerase. PCR products were resolved by agarose gel electrophoresis and visualized by nucleic acid staining.

3.7. Analysis of the genomic integrity of the *IGHM* switch region (Sμ)

Genomic integrity of the immunoglobulin heavy-chain switch-μ (Sμ) region was assessed by PCR amplification of genomic DNA using primers flanking the Sμ locus, to detect potential intra–switch-region deletional events. Genomic DNA was isolated from lymphoma cell lines or primary HGBCL-DH-*BCL2* samples using AllPrep DNA/RNA Mini Kit (Qiagen), following the manufacturer's recommendations, as described in section 3.3. DNA concentration and purity were determined using Qubit dsDNA HS Assay Kit (Thermo Fisher Scientific), NanoDrop 2000/2000c spectrophotometers, and Agilent 2100 Bioanalyzer system and samples were diluted to a working concentration of 20 - 50 ng/μL. For each reaction, up to 100 ng of genomic DNA was used as template in a PCR assay designed to amplify a fragment spanning the Sμ region of the IGH locus. Primers were designed to anneal to conserved sequences flanking the Sμ repetitive region upstream of the constant *IGHM* gene, thereby enabling amplification of the intact genomic interval or any shortened derivatives resulting from deletional events within Sμ. Primer sequences are indicated in table 3. PCR reactions were performed in a total volume of 25 μL, combining 1X GoTaq FLEXI buffer containing 2.5 mM $MgCl_2$, and 1 U thermostable GoTaq Flexi DNA polymerase, 200 μM each dNTP, 0.2 μM of each forward and reverse primer, 1 U thermostable GoTaq Flexi DNA polymerase, and genomic DNA template. PCR products were resolved by electrophoresis on 1.5 - 2% agarose gels prepared in 1× TAE buffer and visualized by nucleic acid staining under ultraviolet illumination. The expected amplicon corresponding to the intact Sμ region was defined based on the reference genomic configuration of the IGH locus, whereas shorter PCR products were interpreted as indicative of intra–Sμ deletions arising from aberrant recombination events. As a negative control for amplification of the Sμ region, genomic DNA derived from IGH^{UND} HGBCL-DH-*BCL2* cases (i.e., lymphomas that had undergone immunoglobulin class-switch recombination and therefore deleted the genomic interval downstream of Sμ) was included in the analysis. PCR products displaying reduced size relative to the expected full-length fragment were excised from the agarose gel using a sterile scalpel and purified with a gel extraction kit. Purified amplicons were subsequently subjected to bidirectional Sanger sequencing using the same PCR primers to characterize the junctions generated by intra–Sμ deletional events and to confirm the presence of deletions within the switch region. Sequencing chromatograms were

analysed using Snapgene alignment software and compared with the reference IGH genomic sequence to identify breakpoint positions and confirm the deletion of internal Sμ segments

3.8. Optimization of RT–PCR-based method for the detection of *CD79B* transcript variants

Alternative splicing of the *CD79B* transcript was assessed by RT–PCR-based approach designed to distinguish the full-length *CD79B* transcript from a splice variant lacking exon 3 ($Ex3^{\Delta}$). Total RNA was extracted from lymphoma cell lines, FACS - purified tonsillar germinal center (GC) B-cell subsets (dark zone, DZ, and light-zone, LZ), and peripheral blood mononuclear cells (PBMCs) obtained from healthy donors, using AllPrep DNA/RNA kit (Qiagen) as described in seciton 3.3., following manufacturer's recommendations. cDNA was synthesized from 0.5 - 1 μg of total RNA using SuperScript III Reverse Transcriptase (Thermo Fisher Scientific) following the manufacturer's instructions as described in section 3.6. cDNA was diluted in nuclease-free water and used as template for PCR amplification. To discriminate between the canonical and alternatively spliced *CD79B* transcripts, PCR primers were designed to anneal to exons located upstream and downstream of exon 3, thereby enabling amplification of both the full-length transcript containing exon 3 (hereafter referred to as Transcript-1, T1) and the shorter exon-skipped transcript lacking exon 3 (Transcript-2, T2). Primer sequences are indicated in table 3. PCR reactions were performed in a total volume of 25 μL containing 1–2 μL of cDNA template, 0.2 μM of each primer, 200 μM dNTPs, 1× PCR buffer with $MgCl_2$, and 1 U thermostable DNA polymerase. Amplified products were resolved by electrophoresis on 2% agarose gels prepared in 1× TAE buffer and visualized using intercalating nucleic acid dye under ultraviolet illumination. PCR parameters were empirically optimized to improve detection sensitivity for the shorter isoform, including adjustment of annealing temperature and cycle number. Amplicons corresponding to both transcript variants were excised from the gel, purified using a gel extraction kit, and subjected to bidirectional Sanger sequencing to confirm exon composition and validate the identity of the amplified splice variants.

3.9. Quantitative RT-PCR analysis of *CD79B* transcript isoforms

Relative expression levels of the *CD79B* transcript variants were quantified using real-time quantitative reverse transcription PCR (RT-qPCR). Total RNA was extracted from lymphoma cell lines and converted into cDNA as described above. Quantitative PCR reactions were performed using isoform-specific primer sets designed to selectively amplify the exon-3–skipped variant (T2), designed across the exon 2–exon 4 junction generated by exon-3

skipping. Exon 4 – exon 5 spanning primers were used to measure overal *CD79B* levels, measuring both T1 and T2 transcript variants. RT-qPCR reactions were carried out in 20 µL volumes using a SYBR Green–based detection system in a real-time PCR thermocycler. Each reaction mixture contained 1× SYBR Green master mix, 0.2 µM of each primer, and 5 µL of diluted cDNA template. Amplification conditions consisted of an initial polymerase activation step at 95 °C for 10 min followed by 45 amplification cycles of denaturation at 95 °C for 10 s and annealing/extension at 60 °C for 10 s. All reactions were performed in technical triplicate, and no-template controls were included to exclude contamination or primer-dimer formation. At the end of the amplification protocol, a melting-curve analysis was performed to verify the specificity of each PCR product. Relative transcript abundance was calculated using the comparative Ct (ΔΔCt) method after normalization to a constitutively expressed housekeeping gene (*GAPDH*). For each cell line, expression levels of the T1 and T2 isoforms were quantified independently and subsequently compared across samples.

Components	**Volume (µl)**
H_2O	13.8
5x GoTaq flexi buffer	5
$MgCl_2$ 25 mM	2
dNTPs 2.5 mM	2
primer Fw 10 µM	0.5
primer Rv 10 µM	0.5
GoTaq Flexi DNA Polymerase	0.2
Template DNA	1
Total	**25**

Table 1. PCR reaction master mix. List of reagents used for individual PCR reactions. Initial concentration for each reagent is indicated

	Temperature (°C)	Time (min)	cycle
Initial denaturation	94	3.00	1
Denaturation	94	0.30	35X
Annealing	T_A	0.30	
Extension	72	0.30	
Final extension	72	5.00	1
Soak	4	hold	

Table 2. Thermal cycling conditions used with GoTaq Flexi DNA Polymerase PCR reactions. Annealing temperature was optimized for each primer set based on the primer T_m

Primer Name	Primer Sequence (5' to 3')	Application
READ1 TS	TCGTCGGCAGCGTCAGATGTGTATAAGAGACAGNNNNNNNNNNNNrGrGrGrGrG	5'RACE
READ1U	TCGTCGGCAGCGTCAGATGTGTATAAGAGACAG	5'RACE
Hu_IgM_RACE_Out	GCCAACGGCCACGCTGCTCGTATCCGA	5'RACE
Hu_IgG_RACE_Out	TCCTGAGGACTGTAGGACAGC	5'RACE
Hu_IgD_RACE_Out	GGTGGTACCCAGTTATCAAGCAT	5'RACE
Hu_IgA_RACE_Out	GGGAAGTTTCTGGCGGTCA	5'RACE
Hu_IgE_RACE_Out	GTGTCCCAGGTCACCATCAC	5'RACE
Hu_IgK_RACE_Out	GGCCTCTCTGGGATAGAAGTTATTCAGCAGGC	5'RACE
Hu_IgL_RACE_Out1	GACACACTAGTGTGGCCTTGTTGGCTTG	5'RACE
Hu_IgL_RACE_Out2	GACACACCAGTGTGGCCTTGTTGGCTTG	5'RACE
Hu_IgL_RACE_Out3	GGCACACCAGTGTGGCCTTGTTGGCTTG	5'RACE
Hu_IgL_RACE_Out4	GACACACCAGCATGGCCTTGTTGGCTTG	5'RACE
Hu_IgM_RACE_In	GTCTCGTGGGCTCGGAGATGTGTATAAGAGACAGGGGAATTCTCACAGGAGACGAGGGGGAAA	5'RACE

Hu_IgG_RACE_In	GTCTCGTGGGCTCGGAGATGTGTATAA GAGACAGAAGACCGATGGGCCCTTG	5’RACE
Hu_IgD_RACE_In	GTCTCGTGGGCTCGGAGATGTGTATAA GAGACAGGGGTGTCTGCACCCTGATA	5’RACE
Hu_IgA_RACE_In	GTCTCGTGGGCTCGGAGATGTGTATAA GAGACAGAAGACCTTGGGGCTGGT	5’RACE
Hu_IgE_RACE_In	GTCTCGTGGGCTCGGAGATGTGTATAA GAGACAGTTGCAGCAGCGGGTCAAGGG	5’RACE
Hu_IgK_RACE_In	GTCTCGTGGGCTCGGAGATGTGTATAA GAGACAGCGGGeAAGATGAAGACAGAT GGTGCAGC	5’RACE
Hu_IgL_RACE_In1	GTCTCGTGGGCTCGGAGATGTGTATAA GAGACAGGAGGAGGGCGGGAACAGAG TGAC	5’RACE
Hu_IgL_RACE_In1	GTCTCGTGGGCTCGGAGATGTGTATAA GAGACAGGAGGAGGGCGGGAACAGAG TGAC	5’RACE
Hu_IgL_RACE_In2	GTCTCGTGGGCTCGGAGATGTGTATAA GAGACAGCAGAGGAGGGTGGGAACAG AGTGAC	5’RACE
N501 F	AATGATACGGCGACCACCGAGATCTAC ACTAGATCGC TCGTCGGCAGCGTC	Sample barcoding
N502 F	AATGATACGGCGACCACCGAGATCTAC ACCTCTCTAT TCGTCGGCAGCGTC	Sample barcoding
N503 F	AATGATACGGCGACCACCGAGATCTAC ACTATCCTCT TCGTCGGCAGCGTC	Sample barcoding
N504 F	AATGATACGGCGACCACCGAGATCTAC ACAGAGTAGA TCGTCGGCAGCGTC	Sample barcoding
N505 F	AATGATACGGCGACCACCGAGATCTAC ACGTAAGGAG TCGTCGGCAGCGTC	Sample barcoding
N506 F	AATGATACGGCGACCACCGAGATCTAC ACACTGCATA TCGTCGGCAGCGTC	Sample barcoding

N507 F	AATGATACGGCGACCACCGAGATCTAC ACAAGGAGTA TCGTCGGCAGCGTC	Sample barcoding
N508 F	AATGATACGGCGACCACCGAGATCTAC ACCTAAGCCT TCGTCGGCAGCGTC	Sample barcoding
N701 R	CAAGCAGAAGACGGCATACGAGATTAA GGCGAGTCTCGTGGGCTCG	Sample barcoding
N702 R	CAAGCAGAAGACGGCATACGAGATCGT ACTAGGTCTCGTGGGCTCG	Sample barcoding
N703 R	CAAGCAGAAGACGGCATACGAGATAGG CAGAAGTCTCGTGGGCTCG	Sample barcoding
N704 R	CAAGCAGAAGACGGCATACGAGATTCC TGAGCGTCTCGTGGGCTCG	Sample barcoding
N705 R	CAAGCAGAAGACGGCATACGAGATGGA CTCCTGTCTCGTGGGCTCG	Sample barcoding
N706 R	CAAGCAGAAGACGGCATACGAGATTAG GCATGGTCTCGTGGGCTCG	Sample barcoding
N707 R	CAAGCAGAAGACGGCATACGAGATCTC TCTACGTCTCGTGGGCTCG	Sample barcoding
N710 R	CAAGCAGAAGACGGCATACGAGATCGA GGCTGGTCTCGTGGGCTCG	Sample barcoding
N711 R	CAAGCAGAAGACGGCATACGAGATAAG AGGCAGTCTCGTGGGCTCG	Sample barcoding
N712 R	CAAGCAGAAGACGGCATACGAGATGTA GAGGAGTCTCGTGGGCTCG	Sample barcoding
N714 R	CAAGCAGAAGACGGCATACGAGATGCT CATGAGTCTCGTGGGCTCG	Sample barcoding
N715 R	CAAGCAGAAGACGGCATACGAGATATC TCAGGGTCTCGTGGGCTCG	Sample barcoding
M-F1	GGAGGGGATGCTCCGGGAAGGTGG	Intra Sμ deletion
M-R1	CGAGGCAGCCAACGGCCACGC	Intra Sμ deletion

Imu F3	GGATGCGTGGCTTCTGCTGC	Detection non-switched sterile transcripts
Imu cons G	TCCTTGACCAGGCAGCCCAG	Detection switched sterile transcripts
Imu cons M	CAACGGCCACGCTGCTCGT	Detection non-switched sterile transcripts
hCD79b_Ex1_FW1	CAGGCTGGCGTTGTCTCC	Detection of *CD79B* transcript variants
hCD79b_qPCR_Ex4_Rev1	TCTGCTTCAGCTGTGCCAAG	Detection of *CD79B* transcript variants
hCD79b_Ex1_FW1	CAGGCTGGCGTTGTCTCC	Detection of *CD79B* transcript variants
hCD79b_Ex6_REV1	GGGTGCTCACCTACAGACCA	Detection of *CD79B* transcript variants
hCD79b_qPCR_Ex3_Fw1	CTCCGGCAATGTGAGCTGG	Detection of *CD79B* transcript variants
hCD79b_qPCR_Ex4_Rev1	TCTGCTTCAGCTGTGCCAAG	Detection of *CD79B* transcript variants
hCD79b_EX2_4 jun fw2	CGGTACCGGAATCCCAAAGGATTC	qRT-PCR primers
hCD79b_EX5 Rev	CTCCATGCCAGCCTTGCTG	qRT-PCR primers
hCD79b_Ex1_Fw2	CTCGGACGTTGTCACGGGT	qRT-PCR primers

hCD79b_EX2_4 Jun Rev	GTGCCAAGGTGCTGAATCCTT	qRT-PCR primers
pax5 f	GATCAGCTACCCCAGCTCGG	qRT-PCR primers
pax5 R	CTGTCCTGCTGGTCCGAGGA	qRT-PCR primers
hCD79b Ex 4 Fw	AGCAGAGGAACACGCTGAAGG	qRT-PCR primers
hCD79b_Ex6_REV1	GGGTGCTCACCTACAGACCA	qRT-PCR primers
GAPDH Fw	AGCGCTGACCTTGAGGTCTCCTTG	qRT-PCR primers
GAPDH Rv		qRT-PCR primers

Table 3. List of primers used in the study. Name of the oligo, sequence (from 5' to 3') and specific application are indicated for each primer.

4. Results

4.1. Overview of Experimental Framework

To comprehensively map the molecular perturbations responsible for the recurrent silencing of BCR expression in HGBCL-DH-*BCL2*, this study implemented a multi-layered investigative strategy focused on three primary regulatory pillars: IGV gene rearrangements, IGH class, and expression of the BCR subunit CD79B.

The experimental workflow began with the reconstruction of clonal IGH and IG light chain V gene rearrangements in HGBCL-DH-*BCL2* retrieved by 5′ rapid amplification of cDNA ends (5′ RACE). Class-specific IGH transcript analysis combined with analyses of the IGH switch-mu genomic region allowed reconstruction of IGH class usage in IGH^{+} and IGH^{UND} HGBCL-DH-*BCL2* cases. Finally, I tested the hypotehsis that BCR silencing in IGH^{UND} HGBCL-DH-*BCl2* resulted from changes in expression and/or transcript isoform usage of the CD79B gene. By integrating these experimental arms across a cohort of primary patient specimens and cell line derivatives, the study has explored three mechanisms potentially responsible for differential IGH expression and IGH class choicc between IGH^{+} and IGH^{UND} HGBCL-DH-*BCL2*.

4.2. IGHV gene profiling in HGBCL-DH-*BCL2* by 5’ rapid amplification of cDNA ends (5’RACE)

To define the molecular architecture of the BCR in HGBCL-DH-*BCL2*, I performed systematic immunoglobulin (IG) profiling across 22 primary clinical cases. We utilized an optimized 5’ Rapid Amplification of cDNA Ends (5’RACE) protocol to capture the complete repertoire of heavy (*IGH*), kappa (*IGK*), and lambda (*IGL*) chain transcripts. The primary advantage of this 5’RACE methodology - summarized in the technical schematic in **Figure 4.2.1** - lies in its ability to amplify full-length *IGH/IGL/IGK* transcripts without prior knowledge of the specific variable (*V*) region utilized by the malignant clone. By employing a template-switching oligonucleotide (TSO) that anneals to the 5' cap of the mRNA during reverse transcription, this method allowed the introduction of a universal adapter sequence functioning as template for subsequent PCR amplification together with locus-specific IG constant region primers. This strategy eliminates the inherent bias of conventional multiplex primer-based amplification, which may fail in HGBCL cases due to the high rate of IG somatic mutations potentiallypreventing primer binding sites.

The robustness of this approach was particularly critical for characterizing IGH^{UND} cases, clones that possess transcriptionally active but highly divergent BCR variants. Successful library preparation was confirmed via agarose gel electrophoresis, which indicated distinct, locus-specific amplicons for *IGH*, *IGK*, and *IGL* across representative HGBCL-DH-*BCL2* cases (**Figure 4.2.2**). Quality check of IG heavy and light chain libraries was confirmed using 2100 Bioanalyzer system, ensuring a narrow, high-quality fragment size distribution suitable for Next-Generation Sequencing (NGS) (**Figure 4.2.3**). The resulting sequencing data revealed a remarkably heterogeneous landscape of light chain usage, as detailed in **Table 4.2.1A**. A pivotal finding emerged from the analysis of IGH^{UND} HGBCL-DH-*BCL2(-BCL6*) cases, most notably in Case #245. Despite its IGH^{UND} phenotype, this case harbored a single, productive, hypermutated *IGHV* gene rearrangement. Conversely, for the same tumor, 5'RACE analyses combind with next generation sequencing of amplicons identified multiple *IGKV* and *IGLV* genes representing both productive and non-productive rearrangements. This result alongside constitutive RAG1/2 expression, is consistent with RAG-dependent IG light chain V-gene editing ongoing within the malignant clone. Similarly, IG light chain V gene profiling of the COH-THL1 cell line established from primary lymphoma cultures of a HGBCL-DH-*BCL2* case (Wang, J.Q. et al., 2019), identified multiple independent rearrangements. This result, combined with the persistent expression in these cells of the *RAG1/2* genes is consistent with a scenario of ongoing IG light chain editing, contributing to the estabslishment of a pool of IGH^{UND} lymphoma cells as a result of the acquistion of non-productive rearrangements. (**Table 4.2.1B**). Collectively, these results indicate that IGH^{UND} HGBCL-DH-*BCL2* frequently exhibit genetic footprints of IG receptor editing, contributing to the extinction of BCR expression.

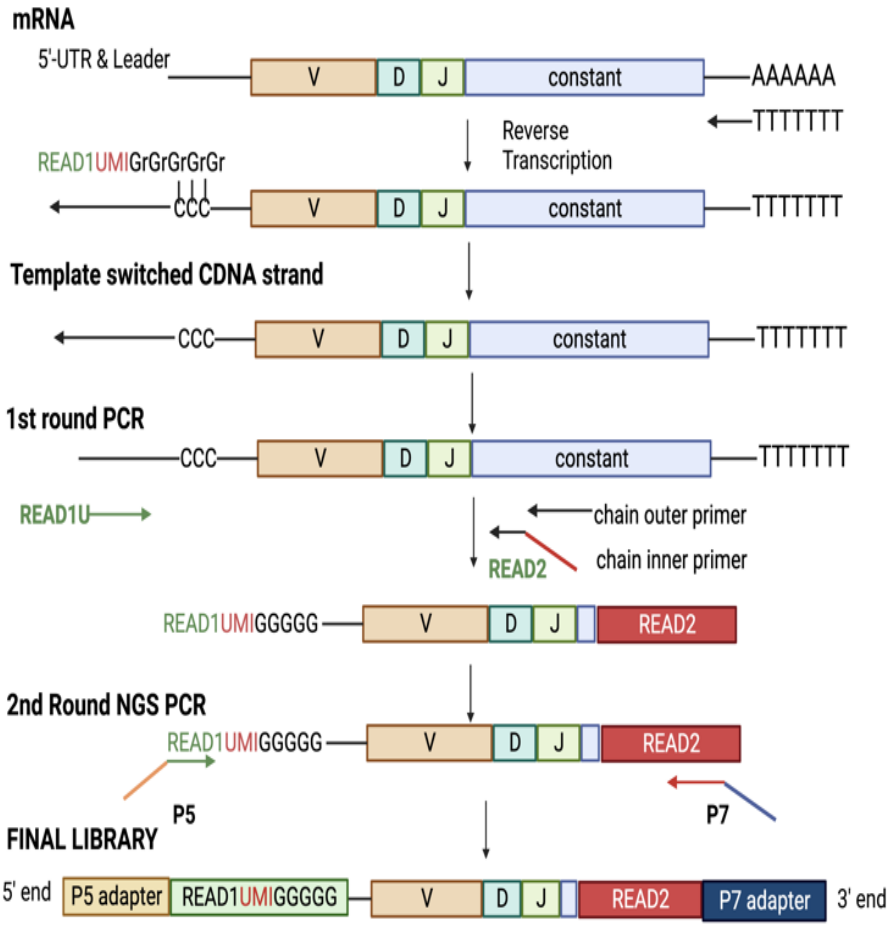

Figure 4.2.1: Schematic overview of the 5′ Rapid Amplification of cDNA Ends (5'RACE) workflow for B-cell receptor repertoire profiling.

During first-strand synthesis, priming with an oligo dT primer captures polyadenylated transcripts and, upon reaching the 5' end of the RNA template, the Reverse Transcriptase Superscript II adds a 5′ poly-cytidine tract upstream of the UTR, to the 3' end of the newly synthesized cDNA strand, providing an anchoring site for a template-switch oligonucleotide (TSO) containing a poly-guanosine RNA stretch of 5 nucleotides (nt) present at the 3' end. The template-switching oligonucleotide (TSO) carries a universal amplification DNA sequence identical to the Illumina's READ1 sequencing primer and a unique molecular identifier (UMI). Upon base pairing between the TSO and the polycytidine stretch, the reverse transcriptase "switches" template strands, and completes cDNA synthesis up to the 5' end of the TSO. The resulting template-switched cDNA containing the READ1-UMI sequence is used for a first round PCR to selectively amplify immunoglobulin transcripts. In this step, a universal forward primer complementary to the template-switch sequence (READ1U) is paired with reverse primers that anneal within the immunoglobulin constant region. A second semi-nested PCR

using inner chain-specific primers containing a 5′ tail identical to the Illumina Read2 sequence primer ensures efficient and specific amplification of the V(D)J-containing amplicons, incorporating the READ1 sequence upstream of the UMI and V segment, while adding the READ2 priming site downstream of the J segment. Finally, adapters and indices suitable for Illumina's MiSeq platform were introduced using a 10-15 cycle PCR step. This approach enables unbiased amplification of the V(D)J repertoire, bypassing the need for V-region specific primers which are often confounded by high somatic hypermutation (SHM) loads in HGBCL-DH-*BCL2* cases. *Abbreviations: UMI, Unique Molecular Identifier; V, Variable; D, Diversity; J, Joining; C, Constant; NGS, Next-Generation Sequencing.*

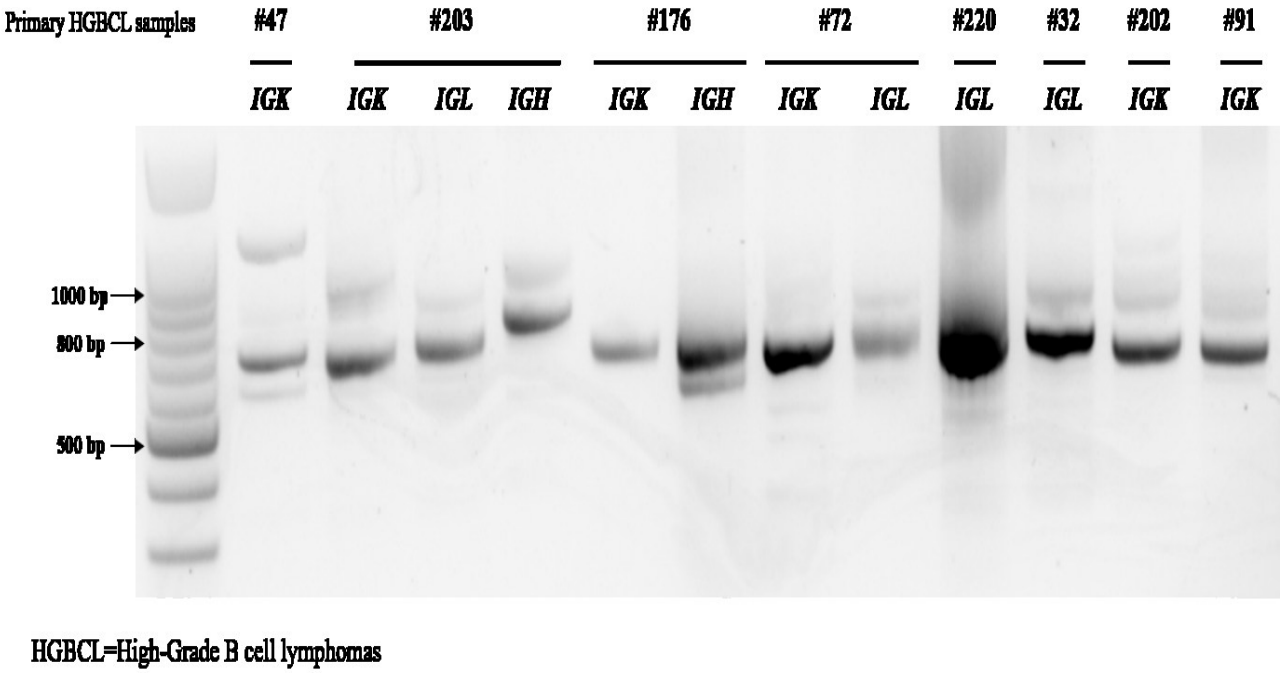

Figure 4.2.2. IG heavy and light chain profiling in primary HGBCL-DH-*BCL2*. Agarose gel electrophoresis (1.5% agarose) of IG heavy (*IGH*) and light (*IGK, IGL*) chain libraries from eight representative primary HGBCL-DH-*BCL2* cases. The expected size for *IGH* and *IGL* chain libraries, including NGS primer and adapter sequences, is ~750 and ~650 bp, respectively. First lane: 100 bp ladder.

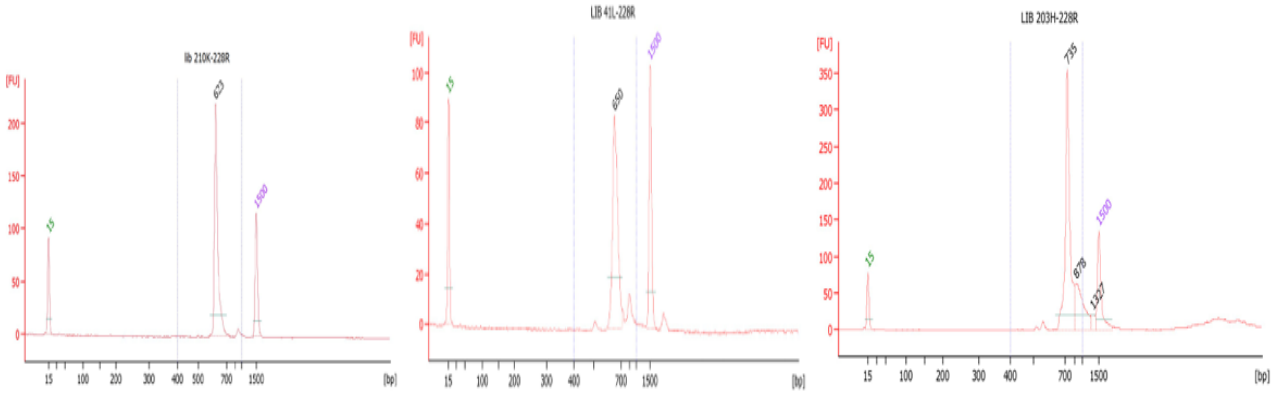

Figure 4.2.3: Quality assessment of 5'RACE libraries

Representative electropherograms showing the quality and size distribution of IG heavy and light chain 5' RACE libraries, analyzed on the Agilent 2100 Bioanalyzer system. The peaks around 650 bp and 735 bp correspond to the IG light chain and heavy chain libraries, respectively, including NGS primers and adapters. The narrow distribution and high fluorescence units (FU) confirmed high-quality, specific amplification suitable for downstream sequencing. Internal lower and upper markers are indicated at 15 bp and 1500 bp, respectively.

ID #	***IGH* (RNA scope)**	**IGH status**	**HGBCL-DH-*BCL2*/ HGBCL-DH-*BCL2-BCL6***	***IGVK* RNA (% of reads)**	***IGJK* RNA**	***IGVK:* Productive**	***IGVL* RNA (% of reads)**	***IGJL* RNA**	***IGVL*: Productive**
235	*IGHM/IGHD*	Positive	HGBCL-DH-*BCL2-BCL6*	*IGKV4-1 (93%)*	*IGKJ2*	Yes	-	-	
53	*IGHM/IGHD/IGHG*	Positive	HGBCL-DH-*BCL2*	*IGKV1-5 (40%)*	*IGKJ1*	-	-	-	-
9	*IGHM*	Positive	HGBCL-DH-*BCL2*	-	-	-	*IGLV1-40 (80%)*	*IGLJ1*	Yes
238	*IGHA*	UND/+	HGBCL-DH-*BCL2*	*IGKV2-28 (50%)*	*IGKJ4*	Yes	*IGLV3-19 (49%)*	*IGLJ2*	Yes
49	*IGHG*	UND/+	HGBCL-DH-*BCL2-BCL6*	*IGKV3-20 (52%)*	*IGKJ1*	Yes	NA	NA	
16	*IGHG*	UND	HGBCL-DH-*BCL2*	-	-	-	*IGLV2-14 (25%)*	*IGLJ1*	Yes

							IGLV1-51 (16%)	*IGLJ7*	Yes
							IGLV2-23 (12%)	*IGLJ3*	Yes
							IGLV3-1 (12%)	*IGLJ2*	Yes
245	*IGHG*	UND	HGBCL-DH-*BCL2-BCL6*	*IGKV4-1 (73%)*	*IGKJ4*	Yes	*IGLV3-1 (36%)*	*IGLJ3*	No
				IGKV2-28 (23%)	*IGKJ3*	No	*IGLV4-3 (29%)*	*IGLJ7*	No
				IGKV2-18 (3%)	*IGKJ4*	No	*IGLV3-10 (28%)*	*IGLJ3*	Yes
				IGKV2-29 (0.5%)	*IGKJ4*	No	*IGLV1-51 (6%)*	*IGLJ3*	Yes
				IGKV2-28 (<0.1%)	*IGKJ4*	Yes	*IGLV2-14*	*IGLJ1*	Yes
305	*IGHG*	UND	HGBCL-DH-*BCL2*	-	-	-	*IGLV1-51 (95%)*	*IGLJ3*	Yes
239	*IGHG*	UND	HGBCL-DH-*BCL2*	-	-	-	*IGLV3-19 (76%)*	*IGLJ2*	Yes
240	*IGHA*	UND	HGBCL-DH-*BCL2*	-	-	-	*IGLV3-19 (34%)*	*IGLJ2*	Yes
							IGLV2-14 (11%)	*IGLJ3*	Yes
							IGLV2-8 (7%)	*IGLJ3*	Yes
							IGLV8-61 (6%)	*IGLJ3*	Yes

Table 4.2.1A: *IGV* gene profiling of IGH^{+} and IGH^{UND} HGBCL-DH-*BCL2(-BCL6)*, revealed by NGS of 5'RACE

Cell line	IG V	Clone ID (#)	Unique counts	Clone (% of reads)	*IGHV*	*IGHJ*	*IGHC*	Germline identity (av. %)	Status
COH-DHL1	*VH*	1	3310	90	*IGHV4-39*	*IGHJ2*	*IGHG1*	87	Productive
	VK	NI	NI	NI	NI	NI	NI	NI	NI
	VL	1	1972	91	*IGLV4-69*	*IGLJ6*	*IGLC6*	99	Non-productive
	VL	3	81	2	*IGLV2-14*	*IGLJ1*	*IGLC1*	95	Productive

Cell line	IG V	Clone ID (#)	Unique counts	Clone (% of reads)	*IGHV*	*IGHJ*	*IGHC*	Germline identity (av. %)	Status
COH-THL1-K	*VH*	1	2973	99	*IGHV4-30-4*	*IGHJ4*	*IGHM*	98	Productive
	VK	3	1011	52	*IGKV3-15*	*IGKJ1*	*IGKC*	95	Productive
	VK	1	630	32	*IGKV4-1*	*IGKJ5*	*IGKC*	99	Productive
	VL	11	298	11	*IGLV2-23*	*IGLJ6*	*IGLC6*	99	Non-productive
	VL	7	343	17	*IGLV3-1*	*IGLJ6*	*IGLC6*	99	Non-productive
	VL	23	51	3	*IGLV3-16*	*IGLJ2*	*IGLC2*	99	Productive
	VL	6	67	4	*IGLV3-27*	*IGLJ3*	*IGLC3*	99	Non-productive
	VL	22	88	5	*IGLV7-43*	*IGLJ6*	*IGLC6*	99	Non-productive
	VL	14	100	5	*IGLV2-34*	*IGLJ1*	*IGLC1*	67	Non-productive

Cell line	IG V	Clone ID (#)	Unique counts	Clone (% of reads)	*IGHV*	*IGHJ*	*IGHC*	Germline identity (av. %)	Status
COH-THL1-L	*VH*	1	756	100	*IGHV4-30-4*	*IGHJ4*	*IGHM*	98	Productive

	VK	2	1679	5	*IGKV4-1*	*IGKJ4*	*IGKC*	99	Non-productive
	VK	6	882	14	*IGKV2-30*	*IGKJ5*	*IGKC*	80	Non-productive
	VK	9	420	11	*IGKV5-2*	*IGKJ2*	*IGKC*	94	Non-productive
	VL	1	949	36	*IGLV2-14*	*IGLJ7*	*IGLC7*	99	Productive
	VL	5	538	21	*IGLV2-23*	*IGLJ2*	*IGLC2*	99	Productive
	VL	6	219	12	*IGLV3-1*	*IGLJ2*	*IGLC2*	99	Productive
	VL	12	291	11	*IGLV2-8*	*IGLJ3*	*IGLC3*	99	Productive
	VL	8	123	7	*IGLV3-10*	*IGLJ2*	*IGLC2*	99	Productive
	VL	17	61	3	*IGLV2-5*	*IGLJ6*	*IGLC6*	99	Non-productive

Cell line	**IGV**	**Clone ID (#)**	**Unique counts**	**Clone (% of reads)**	***IGHV***	***IGHJ***	***IGHC***	**Germline identity (av. %)**	**Status**
COH-THL1-IGH^{UND}	*VH*	1	1562	100	*IGHV4-30-4*	*IGHJ4*	*IGHM*	98	Productive
	VK	7	2435	73	*IGKV2-30*	*IGKJ5*	*IGKC*	80	Non-productive
	VK	1	441	23	*IGKV4-1*	*IGKJ4*	*IGKC*	99	Non-productive
	VK	2	41	2	*IGKV4-1*	*IGKJ4*	*IGKC*	99	Productive
	VK	5	54	1	*IGKV2-30*	*IGKJ5*	*IGKC*	80	Non-productive
	VL	2	214	3	*IGLV2-5*	*IGLJ6*	*IGLC6*	99	Non-productive
	VL	1	111	2	*IGLV2-14*	*IGLJ7*	*IGLC7*	99	Productive
	VL	7	80	13	*IGLV3-10*	*IGLJ6*	*IGLC6*	99	Non-productive
	VL	8	50	8	*IGLV3-1*	*IGLJ6*	*IGLC6*	99	Productive

	VL	6	52	7	*IGLV2-23*	*IGLJ6*	*IGLC6*	99	Productive

Table 4.2.1B. *IGV* gene profiling of IGH^{UND} COH-DHL1 and IGK^{+}, IGL^{+} and IGH^{UND} COH-THL1 lines, analyzed by 5'RACE, followed by NGS of PCR amplicons. [NI=not identified]

4.3. IGH class informs on the cell-of-origin of IGH^{+} and IGH^{UND} HGBCL-DH-*BCL2*

A critical challenge in HGBCL is the high frequency of cases bearing the IGH^{UND} phenotype, precluding the possibility to enquire the IGH class selected by the malignant B cells. Building on recent findings from the host laboratory (Varano et al., *BCD* 2025), which utilized RNAscope technology to show that IGH^{UND} cases retain expression of IGH transcripts, I aimed to determine whether IGH protein silencing was linked to a particular IGH class selected by the lymphoma precursor cell and conserved throughout cell transformation. As shown in the in **Figure 4.3.1**, I designed an RT-PCR-based gene expression assay to measure IGH sterile transcripts. This approach combines a forward primer annealing to the Iμ sterile exon mapping upstream to the first IGH constant region gene (*IGHM)* matched to a reverse primer annealing to individual IGH constant region genes starting from *IGHM* and continuing along the chromosome in a 5' to 3' direction with *IGHD*, *IGHG3*, *IGHG1*, *IGHA1*, *IGHG2*, *IGHG4*, *IGHE* and *IGHA2.* Upon IGH CSR the IGHM gene is deleted and rteplaced by a downstream IGH constant region gene. In this setting IG CSR is accompanied by the absence of the Iμ-*IGHM* sterile transcript substituted by an alternative transcript consisting of the Iμ sterile exon spliced to one of the downstream IGH constant region genes (i.e. Iμ-IGHG1 in B cells expressing the IgG1 heavy chain),

The IGH sterile transcript RT-PCR assay was optimized on a panel of DLBCL cell lines with known IGH isotype profile including WSU-DLCL2 (IGG^{+}), SUDHL4 (IGG^{+}), and OCI-LY7 (IGM^{+}) cells. As shown in **Figure 4.3.2**, this optimization step allowed for the identification of the most efficient primer pairs, yielding highly specific amplicons discriminating IGM from IGG transcripts. Next, we applied the IGH RT-PCR assay to the patient-derived HGBCL-DH-*BCL2* cell line models COH-THL1 (IGM^{+}) and COH-DHL1 (IGH^{UND}). (**Figure 4.3.3**): While amplification of IGH sterile transcripts from the COH-THL1 model identified an IGM-specific RT-PCR product, IGH^{UND} COH-DHL1 cells expressed IGG sterile transcripts.

These results align with data shown in Varano et al., indicating that IGH^{+} HGBCL-DH-*BCL2* preferentially (93% of the cases) express the IGM isotype, while the IGH^{UND} counterparts primarily (95% of the cases) express IGH-switched IGG or IGA transcripts.

Collectively, these findings indicate that whereas BCR+ HGBCl-DH-*BCL2* predominantly originate from IGM-expressing GC B cells, their IGH^{UND} counterparts arose from GC B cells which had completed IGH CSR.

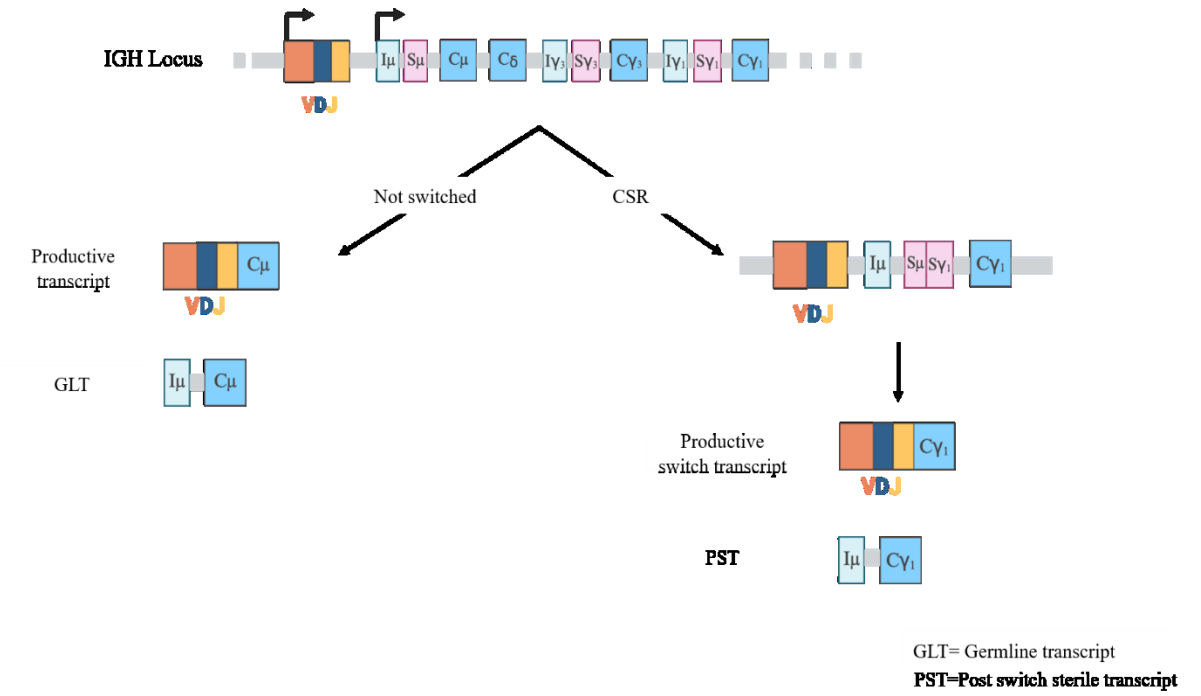

Figure 4.3.1: Schematic representation of the *IGH* locus before and after undergoing class-switch recombination (CSR).

In unswitched human B cells, IG heavy chain locus contains the rearranged variable region (VDJ) followed by the constant region genes encoding IgM (Cμ), IgD (Cδ), IgG3 (Cγ3), IgG1 (Cγ1), IgA1 (Cα), IgG2 (Cγ2), and IgG4 (γ4). Each constant region is preceded by a switch (S) region (e. g., Sμ, Sγ1, etc) and a sterile exon (Iμ, Iγ3, Iγ1, etc), which drives transcription of sterile germline transcripts (GLTs). Transcription from these sterile exons promotes chromatin accessibility and enable targeting by the activation-induced cytidine deaminase (AID), which initiates recombination between switch regions. This process results in the excision of the intervening DNA and juxtaposition of the VDJ exon with a downstream constant region. During class-switch recombination from IgM (left) to IgG1 (right), the Cμ, Cδ, and Cγ3 genes are excised, allowing the VDJ exon to be spliced to Cγ1, resulting in the expression of post-switch transcripts.

RT-PCR strategies using forward primers annealing to the Iμ sterile exon and reverse primers targeting specific constant region genes can distinguish unswitched from switched cells. In

unswitched cells, the Iμ–Cμ primer pair amplifies the corresponding germline transcript. After CSR to IgG1, the Cμ region is deleted while the Iμ exon is retained; therefore, amplification occurs only when the Iμ forward primer is paired with an IGHG1 reverse primer, indicating successful class switching.

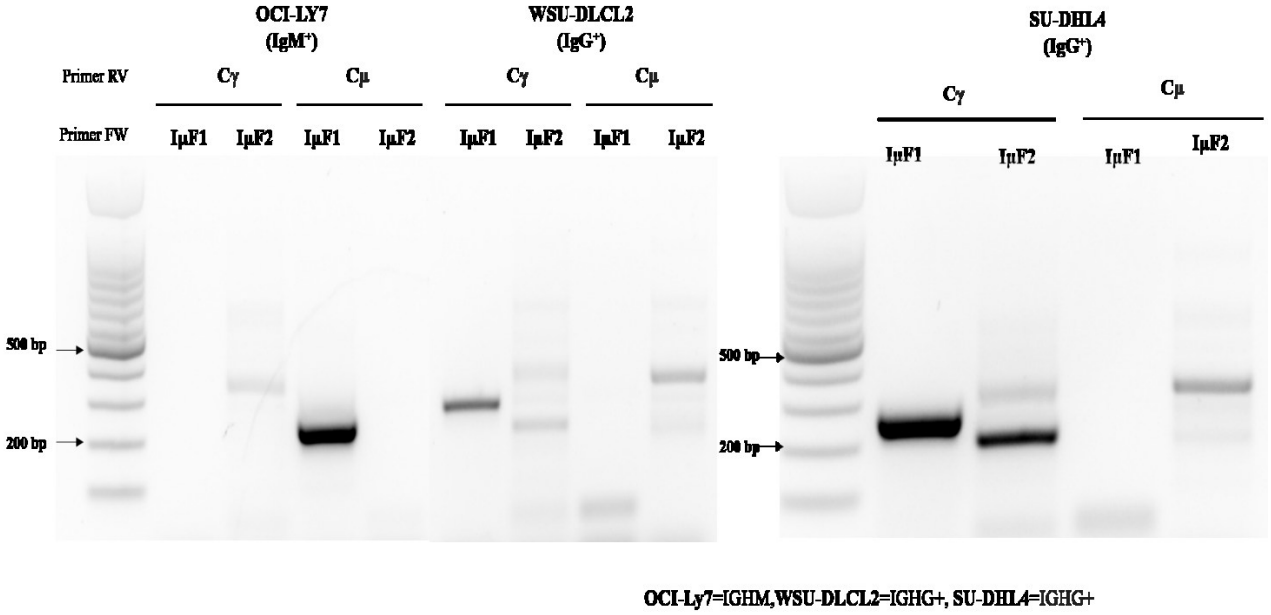

Figure 4.3.2: RT-PCR assay for the detection of post-switch transcripts.

Agarose gel electrophoresis showing amplification of germline transcripts (GLT, *IGM*) or post-switch transcripts (PST, *IGHG1*) in IgM+ or IgG+ Diffuse Large B cell lymphoma (DLBCL) cell lines, respectively, using isotype-specific primer pairs (as described in figure 4.3.1). RT-PCR was performed using Iμ forward primers (F1, F2) in combination with reverse primers for Cμ (IgM) or Cγ1 (IgG) constant regions. The Iμ–Cμ amplicon corresponding to the IgM germline transcript was detected in the IgM^+ OCI-LY7 cell line (Iμ F1 paired with the Cμ reverse primer). In contrast, only non-specific bands (*) were observed in the IgG^+ WSU-DLBCL2 and SUDHL4 cell lines with this primer pair, consistent with deletion of the Cμ region following class-switch recombination. Conversely, Cγ1-specific post-switch transcripts were detected exclusively in the IgG^+ WSU-DLCL2 and SUDHL4 cell lines when the Iμ forward primer was paired with the Cγ1 reverse primer, confirming the specificity of the assay for detecting class-switched transcripts

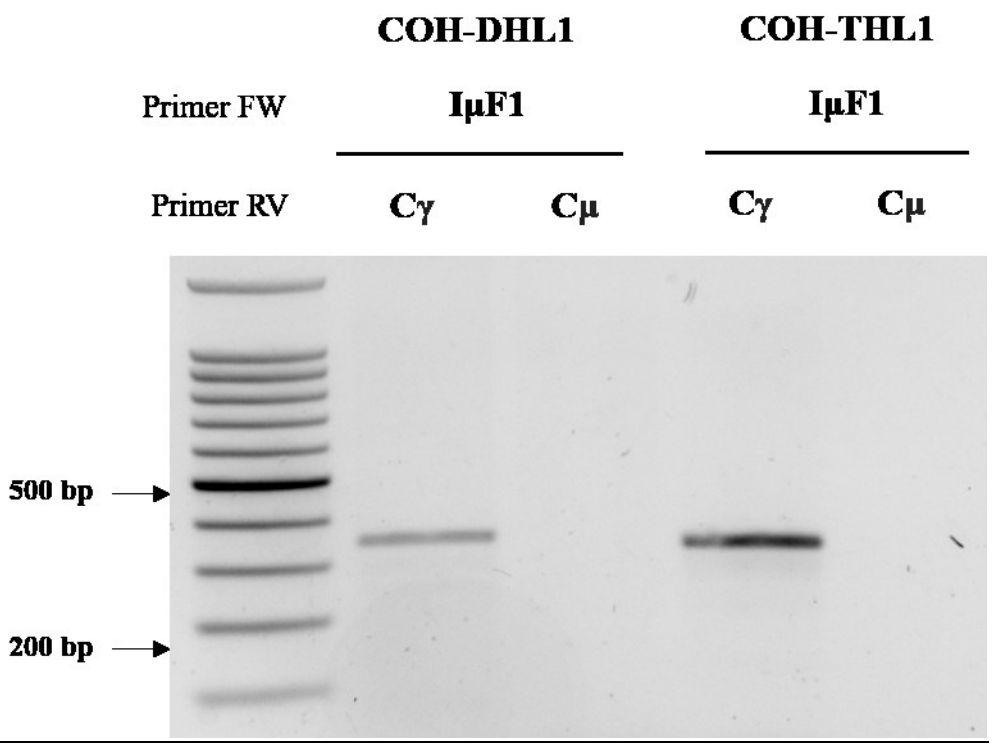

Figure 4.3.3: Analysis of IGH isotype usage in HGBCL-DH-*BCL2* cell lines.
Agarose gel electrophoresis showing IGH isotype in the COH-DHL1 and COH-THL1 cell lines, by RT-PCR analysis of sterile transcripts. RT–PCR was performed using a forward primer annealing to the Iμ sterile exon in combination with reverse primers targeting individual constant region genes. The IGH^{UND} cell line COH-DHL1 displays a specific Iμ–Cγ amplicon, consistent with class-switch recombination to the IgG isotype. In contrast, the IgH^{+} COH-THL1 (THL) cell line shows an Iμ–Cμ–specific amplicon, indicating retention of a pre-switch IgM isotype. No amplification of Iμ–Cδ (IgD) or Iμ–Cμ (IgM) transcripts was detected in the COH-DHL1 sample, and no Iμ–Cδ amplification was observed in the COH-THL1 sample, confirming the specificity of the detected isotype-associated transcriptional profiles in these representative HGBCL models.

4.4. Why do BCR+ HGBCL-DH-*BCL2* fail to undergo IG CSR?

We next asked how IGM-expressing HGBCL-DH-*BCL2* experiencing AID expression evaded IG CSR. To investigate this, we monitored the integrity of the IGH switch-μ (Sμ) genomic region, which is targeted by AID to initiate the process of IG CSR, promoting staggered double stranded DNA breaks. Similar breaks are also introduced in a switch region proximal to a downstream IGH constant region gene (i.e. *IGHG1*). Simultaneous breaks at the two IGH switch regions favors the deletion of the intervening genomic DNA and rejoining of the IGH

locus placing the proximal *IGHV* gene in proximity to a distal IGH constant region gene. The process of IG CSR may however fail leading to the reconstitution of the Smu region. In an attempt to investigate the status of the Sμ region in IGM expressing HGBCL-DH-*BCL2*, I performed a genomic PCR using primers flanking this region to amplify DNA from representative cases. Notably, as shown in **Figure 4.4.1** 5 out of 9 (56%) IGM^{+} lymphomas showed shorter Sμ amplicons compatible with intra Sμ deletional events. IGH^{UND} cases, which completed IGh CSR, and thereby deleted the genomic region downstream to Sμ acted as negative controls. Shorter Sμ genomic regions amplified from IGM^{+} cases were subjected to Sanger sequencing confirming deletional events, Collectively, these findings support a scenario whereby a fraction of HGBCL-DH-*BCL2* cases remain strictly dependent on IGM expression. To achieve this precursor of lymphoma, extended to their malignant derivatives, are selected on the basis of repeated failures of IGH CSR leading to the progressive erosion of the Sμ region, utlimately precluding replacement of IGM with a class-switched IGG/IGA alternative. In a context of chronic BCR signaling we hypothesize that IGM expression, but not IG-switched BCRs, may provide a specific signaling "threshold" optimal for tumor survival. Recognition of a self-antigen within the microenvironment may drive such chronic stimulation; however, surface expression of a switched isotype (such as IGG), which possesses a different cytoplasmic tail and signaling potency, might trigger an excessively strong signal that is incompatible with cellular fitness or leads to activation-induced apoptosis. Extending this logic, we propose that the IGH^{UND} phenotype may represent a further evolutionary step in this signaling continuum. In these cases, the transition to a switched isotype may have indeed generated a "too strong" chronic signal, prompting the malignant clone to silence its BCR expression entirely, thereby "learning" its way out of signaling-induced toxicity while maintaining alternative survival pathways. This creates a distinct biological bifurcation: IGM+ clones that survive by structurally preventing isotype switch, while IGH^{UND} tumors surviving by silencing a potentially deleterious switched receptor.

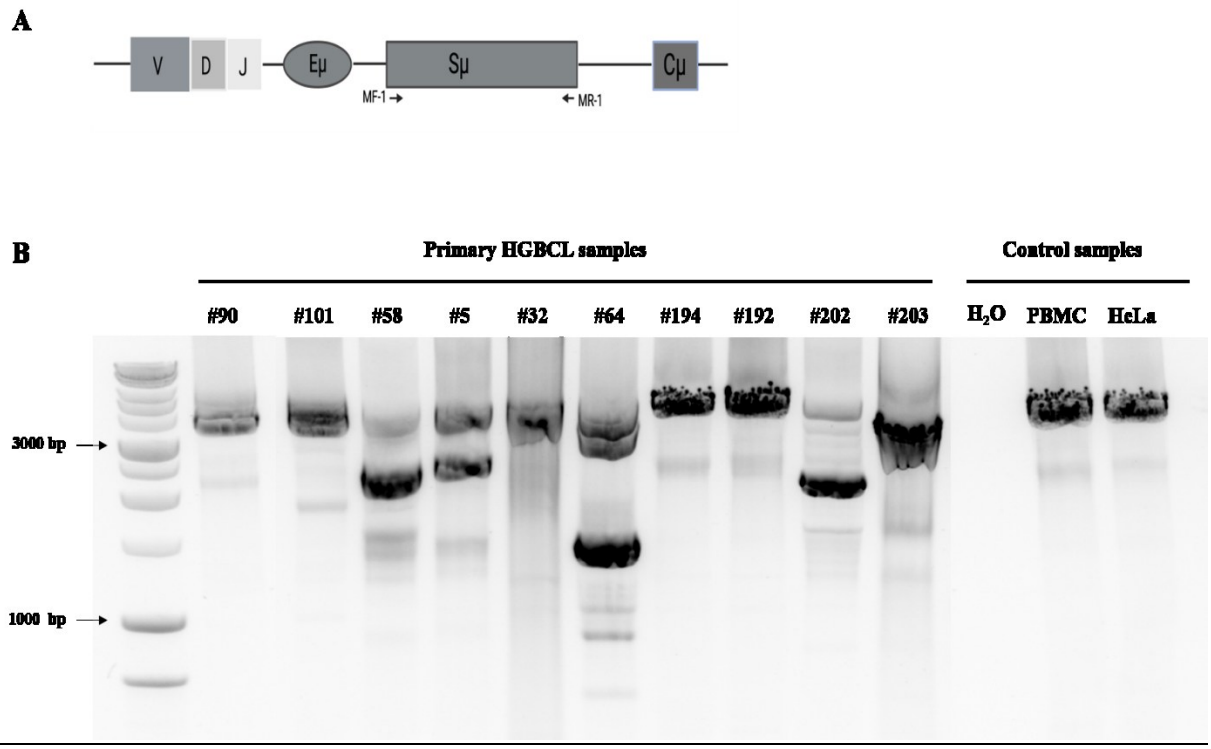

Figure 4.4.1. Analysis of deletions within the Sμ region in primary HGBCL-DH-*BCL2* cases. A. Schematic representation of the Sμ switch region within the IGH locus. The positions of the primers flanking the Sμ region used for genomic PCR amplification are indicated. **B.** Agarose gel electrophoresis of genomic PCR products spanning the Sμ switch region in representative HGBCL-DH-*BCL2* primary cases. Control samples (PBMCs and Hela non-B cells) dissplay the expected full-length Sμ amplicon (upper bands). In contrast, several IgM+cases (eg, #58, #5, #64, #202) show additional low-molecular weight amplicons. These truncated products are consistent with internal deletions within the Sμ region, which likely disrupt structural integrity of the switch region and thereby prevent class-switch recombination to downstream constant. Region genes, while mantaining constitutive IgM expression.

4.5. IG-independent routes to BCR silencing in IGH^{UND} HGBCL-DH-*BCL2*

4.5.1. CD79B protein is recurrently downregulated in IGH^{UND} HGBCL-DH-*BCL2*

Expression of a functional BCR strictly depends on the assembly of a complex between IGH/L chains and the CD79A/B sububnits. Failed expression of any of the BCR components favors clearance of the remaining ones (or extracellular secretion in the case of the IG light chain). Therefore, we hypothesized that failure to detect IGH protein in BCR-silenced HGBCL-DH-*BCL2* could be linked to silencing of the CD79B protein. In line with this scenario, work performed in the hosting lab with the help of collaborators, revealed that IGH^{UND} HGBCL-DH-*BCL2* frequently exhibit reduction in CD79B abundance accompanied by intracellular retention of the protein and failure to form complexes with residual traces of IGH protein (Varano et al. BCD 2025). These results questioned a possible mechanism responsible for CD79B downregulation in IGH^{UND} HGBCL-DH-*BCL2* cases.

4.5.2. Tracking alternative splicing of the CD79B gene in normal and malignant B cells

To explore whether alternative splicing could be responsible for reduced CD79B protein expression in IGH^{UND} HGBCL-DH-*BCL2*, we focused on a particular mRNA isoform skipping exon-3 (Ex3$^{\Delta}$). The *CD79B$^{Ex3\Delta}$* isoform lacks the sequence encoding for the extracellular immunoglobulin-like (Ig-like) domain, a region critical for the non-covalent association between the CD79A/B heterodimer and the IGH chain. Expression of the *CD79B$^{Ex3\Delta}$* isoform is associated with significantly impaired surface BCR expression in chronic lymphocytic leukemia (Alfarano et al., 1999,) To monitor CD79B isoform expression in HGBCL-DH-BCL2, we designed an RT-PCR protocol using primers annealing respectively to exons upstream and downstream of exon 3, as detailed in Figure 4.5.2.1. This approach allows for the simultaneous detection of the full-length transcript and the shorter Ex3$^{\Delta}$ isoform.

The experimental workflow was optimized measuring CD79B transcripts in peripheral blood mononuclear cells (PBMC) from healthy donors. Agarose gel electrophoresis of amplified transcripts identified a larger fragment corresponding to full-length CD79B (hereafter called Transcript-1 or T1) and a shorter fragment (Transcript-2 or T2) corresponding to the Ex3$^{\Delta}$ variant which became more apparent after rigorous optimization of the PCR parameters (Figure 4.4.2.2). Identity of T1 and T2 transcripts was confirmed by Sanger sequencing of the amplified RT-PCR product. Next, we analyzed the CD79B T1/T2 transcript pattern in primary FACS-

sorted tonsillar GC DZ and LZ B cells previously isolated by the hosting lab, alongside DLBCL cell lines.

Intriguingly, while both the Ex3$^{\Delta}$ variant was expressed also in non-transformed DZ B cells, the presumed cell of origin (COO) for HGBCL-DH-BCL2, (Figure 4.4.2.3). The identification of this variant in the DZ suggests that CD79B alternative splicing may be a physiologic mechanism used by proliferating B cells to modulate BCR levels during somatic hypermutation.

These results suggest that alternative splicing of the *CD79B* gene represents a possible mechanism operating in normal and malignant GC DZ B cells to reduce the expression level of the CD79B protein, thereby contributing to the silencing of BCR expression. These results layed the ground to investigate CD79B transcript isoform usage in HGBCL-DH-*BCL2*.

4.5.3. Quantitative assessment of CD79B T1 and T2 transcripts in HGBCL-DH-*BCL2* models

To quantify levels of *CD79B* T1 and T2 mRNA isoforms, we performed quantitative RT-qPCR screening both of IGH+ and IGH^{UND} HGBCL-DH-*BCL2* cell lines. CD79B T1 levels varied substantially across the investigated lines, showing no correlation with sBCR levels (Figure 4.5.2.4). Similarly, while the T2 transcript was detected in roughly half of the cell line models, it did not positively correlate with sBCR extinction (Figure 4.5.2.4). These results suggest that the "BCR-silent" phenotype in IGH^{UND} cases is not primarily caused by preferential *CD79B* exon-3 skipping or upregulation of the *CD79B* T2 isoform.

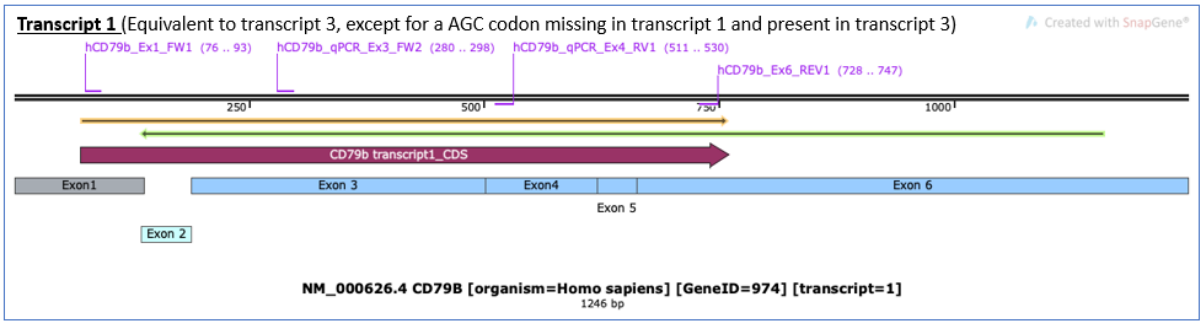

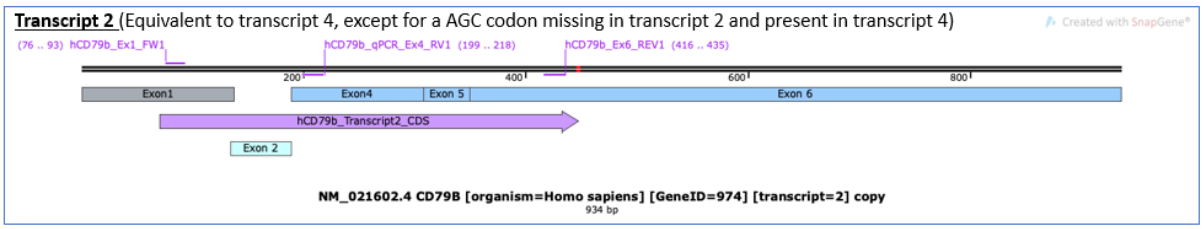

Figure 4.5.2.1: Alternative transcript variants of human *CD79B* gene. Schematic representation of the two major CD79B transcript variants: the full-length transcript (Transcript 1, T1) and an exon 3–skipped isoform (Transcript 2, T2). Transcript 1 corresponds to the canonical mRNA and includes exon 3, which encodes the extracellular immunoglobulin-like domain required for proper B-cell receptor (BCR) assembly and surface expression. Transcript 2 results from alternative splicing that skips exon 3 (ΔEx3), generating a shorter isoform associated with impaired surface BCR expression.

Purple annotations indicate the primer design strategy used for transcript detection. A forward primer located in exon 1 and a reverse primer in exon 6 allow simultaneous amplification of both transcript variants by RT–PCR, enabling discrimination based on amplicon size. In addition, internal qPCR primer pairs were designed to specifically quantify the full-length transcript.

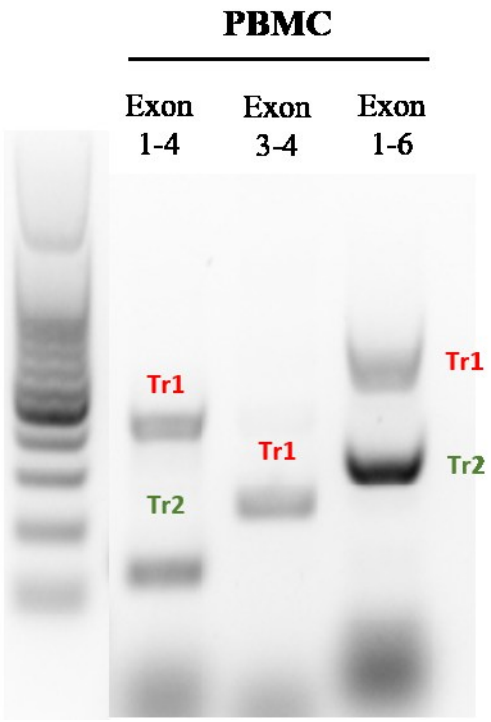

Predicted MW amplicons for Transcript 1 or Transcript 2:

Ex1/Ex4: T1=455 vs T2= 143bp

Ex3/Ex4: T1=251 vs T2= No amplification

Ex1/Ex6: T1=672 vs T2= 360bp

Figure 4.5.2.2: Optimization of an RT-PCR strategy for detecting CD79B alternative splicing variants.

Agarose gel electrophoresis of RT–PCR products corresponding to the full-length *CD79B* transcript (Transcript 1, T1) and the exon 3–skipped variant (Transcript 2, T2), measured in peripheral blood mononuclear cells (PBMCs). Discrimination between the two isoforms was achieved using multiple primer combinations targeting different exon junctions.

Amplification with primers spanning exon 1–4 and exon 1–6 produced two distinct bands corresponding to the predicted sizes of the full-length transcript (T1; ~455 bp and ~672 bp,

respectively) and the exon 3–skipped variant (T2; ~143 bp and ~360 bp, respectively). In contrast, amplification with primers spanning exon 3–4 generated a single band corresponding exclusively to T1.

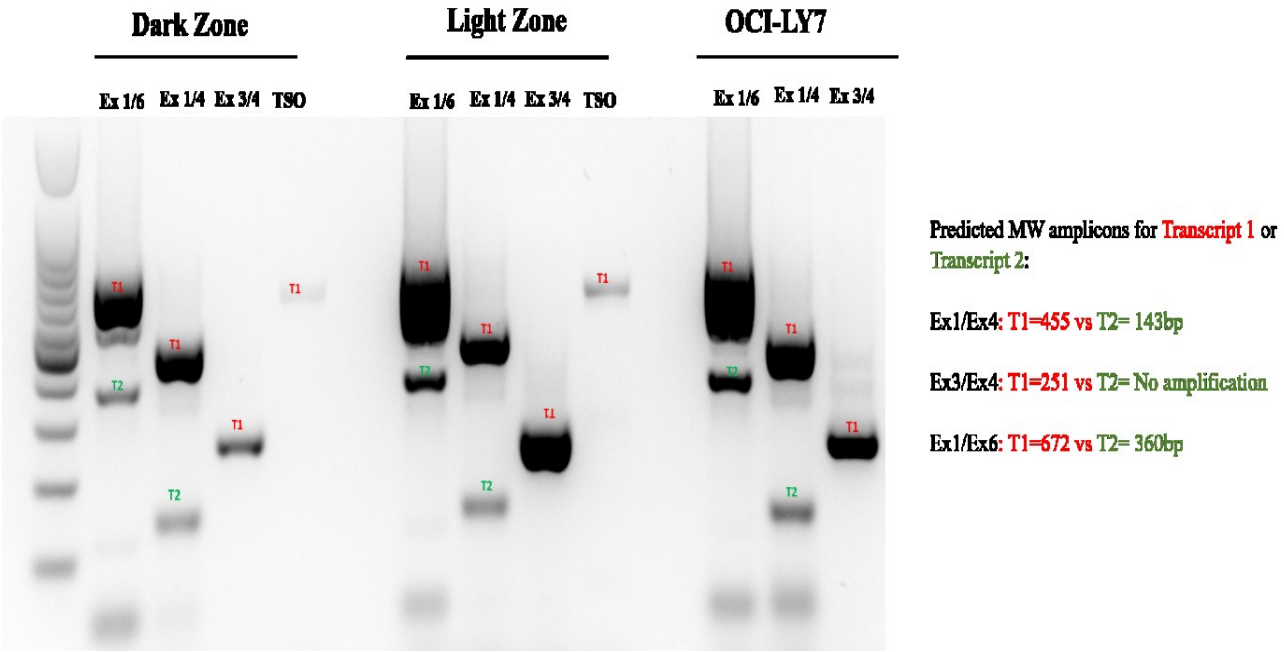

Figure 4.5.2.3: Analysis of the expression of *CD79B* transcript variants in dark-zone and light-zone germinal center B cells. PCR amplification of *CD79B* transcript variants using exon-specific primers. T1 and T2 *CD79B* transcript variants yielded distinct fragment sizes, indicating that both isoforms can be simultaneously express multiple in germinal center B cell subsets, potentially modulating the strength, quality, or localisation of BCR signalling.

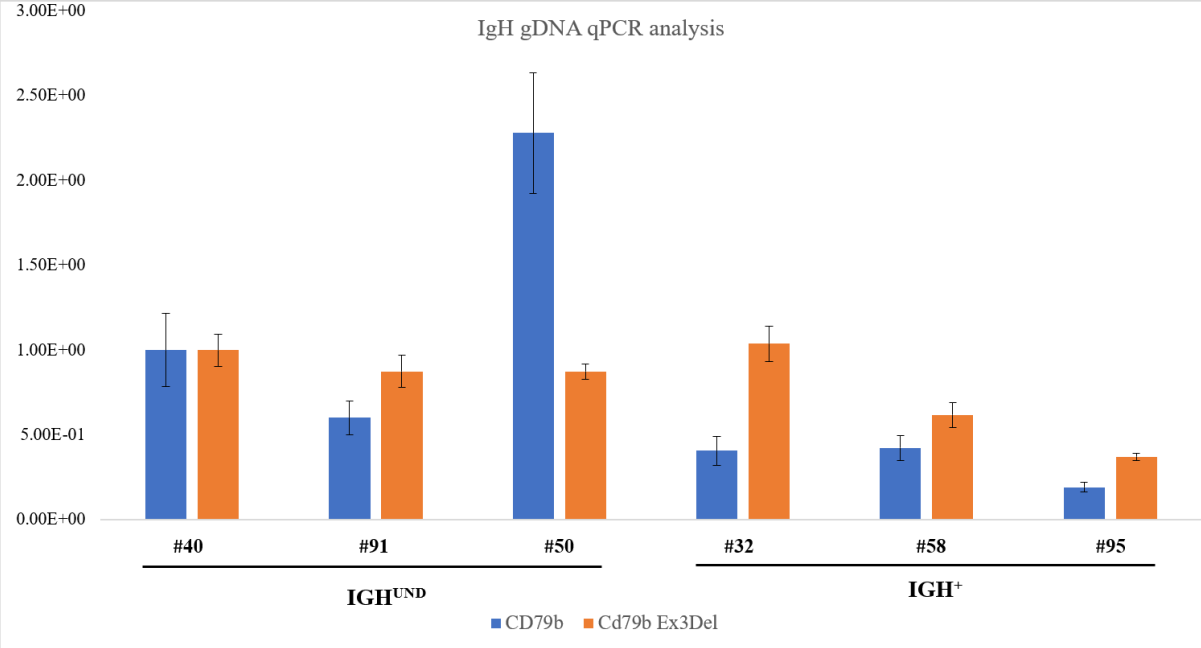

Figure 4.5.2.4: Expression of CD79B transcript variants in HGBCL-DH-*BCL2* primary cases.

Quantitative RT-PCR (qRT-PCR) analysis of *CD79B* transcript variants in IGH+ and IGH^{UND} HGBCL-DH-*BCL2* cases. Expression levels of the full-length transcript (T1; blue bars) and the exon 3–skipped isoform (CD79B Ex3Del; orange bars) reveal heterogeneous expression of both variants across all samples analyzed, irrespective of IGH status. Data are shown as the mean of $n = 3$ technical replicates ± standard deviation.

5. Discussion

5.1. Overview of key findings and biological context

This study provides an integrated molecular dissection of BCR silencing in HGBCL-DH-*BCL2* by combining analyses of IG V gene configuration, IGH class usage, and *CD79B* expression. The results reveal that loss of BCR expression is not attributable to a single genetic lesion, but rather reflects alternative, not necessarily mutually exclusive mechanisms linked to the developmental origin and evolutionary trajectory of the malignant clone.

Three principal conclusions emerge. First, BCR-silenced, IGH^{UND} lymphomas retain potentially productive IGH V gene rearrangements, excluding crippling mutations as a general mechanism of BCR silencing. Second, IGH class usage segregates strongly with BCR expression status, with IGH^{UND} HGBCL-DH-*BCL2* predominantly transcribing IGH class-switched genes, whereas BCR-positive cases preferentially retain IGM expression. Third, although *CD79B* gene expression is variable across tumors, alternative splicing does not appear to represent a dominant mechanism underlying CD79B downregulation in IGH^{UND} HGBCL-DH-*BCL2* cases. =

Collectively, these findings support a model in which BCR expression in HGBCL-DH-*BCL2* reflects distinct biological states associated with differential reliance on sBCR signals, ultimately modulating the evolutionary trajectory of each individual malignant B cell.

5.2. IGV gene analysis reveals productive IGH rearrangements and footprints of receptor editing in IGH^{UND} HGBCL-DH-*BCL2*

A central finding of my work is that IGH^{UND} lymphomas consistently retain productive *IGHV* rearrangements. This observation argues against the hypothesis that BCR loss is primarily driven by crippling mutations as observed in classical Hodgkin Lymphoma (Varano *et al.* 2025) Instead, the detection of multiple productive and non-productive IG light chain rearrangements provides strong evidence for receptor editing activity. This process, normally confined to early B cell development, appears to be aberrantly reactivated in these tumors, likely through re-expression of the *RAG1/2* recombinase genes.

Together, our findings support a model in which defective receptor assembly, rather than genetic inactivation of IGH, underlies BCR silencing in IGH^{UND} HGBCL-DH-*BCL2*.

5.3. IGH class usage is skewed toward class-switched isotypes in IGH^{UND} HGBCL-DH-*BCL2*

Another major finding linked to my work is the association between IGH class usage and BCR expression status. IGH^{UND} lymphomas predominantly express IGH class-switched transcripts (IGG or IGA), whereas BCR-positive tumors largely retain IgM expression. This dichotomy provides important insight into the cell of origin of these tumors. IGH^{UND} lymphomas likely derive from GC B cells that have completed IG CSR, whereas BCR-positive cases primarily arise from cells that have failed or been selected against completing IG CSR.

IGH class switching is associated with qualitative and quantitative changes in BCR signalling. It is therefore plausible that the acquisition of an IGH switched BCR may generate a signalling environment that is incompatible with sustained surface BCR expression in specific oncogenic contexts associated with the outgrowth of IGH^{UND} HGBCL-DH-*BCL2*, favouring instead receptor silencing.

5.4. BCR-positive HGBCL-DH-*BCL2* maintain IGM expression through "erosion" of IGH switch-μ genomic regions

The identification of deletions within the IGH switch-μ (Sμ) region in IGM-expressing HGBCL-DH-*BCL2* provides a mechanistic explanation for their failure to complete IG CSR. These structural alterations are expected to impair AID-initiated IGH class switching, thereby enforcing IGM expression.

This observation supports the existence of selective pressure favouring maintenance of IGM-based BCR signalling. IGM BCRs deliver signalling outputs that differ quantitatively and qualitatively from IGH class-switched receptors, potentially providing an optimal signalling threshold necessary for the genesis and possibly maintenance of IGH^{+} HGBCL-DH-*BCL2* cases.

Our work supports a model whereby IGM-dependent lymphoma precursor cells may be selected for repeated failed CSR events, progressively eroding the Sμ region and thereby locking the malignant clone into an IGM-expressing state. Conversely, IGH^{UND} lymphomas may have followed a strikingly different evolutionary route, during which complete BCR silencing allows escape from signalling states that are no longer compatible with optimal tumour fitness.

5.5. The CD79B gene shows evidence of alternative splicing in HGBCL-DH-*BCL2* models, including an exon-3-deleted isoform associated with impaired BCR assembly

Analysis of *CD79B* transcripts in HGBCL-DH-*BCL2* cell line models revealed the presence of alternatively spliced isoforms, including an exon-3–deleted variant lacking the extracellular immunoglobulin-like domain required for interaction with IGH. Notably, this isoform is not restricted to malignant cells but is also detectable in normal GC DZ B cells. This observation suggests that alternative splicing of CD79B in HGBCL-DH-*BCL2* may represent a mechanism hijacked by malignant B cells from normal germinal center B cells to transiently downregulate BCR expression during rapid proliferation in the dark zone.

5.6. The CD79B exon-3-deleted isoform does not correlate with the IGHUND phenotype

Despite its potential functional relevance, quantitative transcript measurements did not reveal a clear association between expression of the exon-3–deleted *CD79B* isoform and BCR silencing. Both full-length and truncated transcripts were variably expressed across IGH-positive and IGH^{UND} HGBCL-DH-*BCL2* models, indicating that alternative splicing alone is insufficient to account for the IGH^{UND} phenotype. These findings suggest that mechanisms operating beyond regulation of CD79B gene expression and splicing are responsible for the reduced protein levels observed in IGH^{UND} lymphomas.

5.7. Mechanisms of BCR silencing in HGBCL-DH-*BCL2*

The work presented in this thesis is part of a broader and more comprehensive effort carried out by the hosting laboratory to elucidate the mechanisms responsible for BCR silencing in IGH^{UND} HGBCL-DH-*BCL2*. Based on the full complement of experimental evidence accumulated by the lab, we propose several non-mutually exclusive scenarios that may account for BCR silencing in the majority of HGBCL-DH-*BCL2* cases.

1.Receptor editing and IG light chain diversification. Reactivation of RAG1/2 expression and recombinase activity promotes ongoing IG light chain V gene recombination, leading to the accumulation of non-productive rearrangements or the generation of light chains unable to efficiently pair with the pre-existing IGH chain. As a consequence, BCR assembly is disrupted,

resulting in the targeting of unpaired immunoglobulin chains and CD79B for intracellular degradation.

2. Impaired folding and stability of hypermutated IGH chains**.** Although IGH transcripts are productive, extensive V gene somatic mutation may compromise proper folding of the encoded proteins. Misfolded IGH chains are likely retained within the endoplasmic reticulum and targeted for degradation, thereby preventing surface expression.

3. Post-transcriptional and post-translational regulation of CD79B. While this study excludes a major role for alternative splicing in CD79B downregulation, it does not rule out regulation at the protein level. In this context, the adaptor protein KLHL4 has recently emerged as a key regulator of CD79B stability through ubiquitin-mediated degradation pathways in mature B-cell lymphomas (Choi *et al.* 2020) Increased activity of such pathways could reduce steady-state CD79B protein levels, thereby impairing BCR assembly and surface expression. Notably, reduced CD79B protein abundance is also a physiological feature of GC DZ B cells, suggesting that malignant cells may exploit conserved regulatory programs controlling receptor turnover.

5.8. Clinical implications

The identification by our lab of a predominant fraction of BCR-silenced HGBCL-DH-*BCL2* cases has direct therapeutic implications. The antibody-drug conjugate Polatuzumab vedotin (pola-V) relies on surface CD79B expression on target cells for effective targeting and internalization of a cytotoxic paylod (Camus & Tilly ,2021). Loss of BCR/CD79B expression is therefore expected to confer intrinsic resistance to these therapies. Our findings support the need to assess IGH status at diagnosis. In particular, patients with IGH^{UND} lymphomas may benefit from Pola-V–free treatment strategies, thereby avoiding unnecessary exposure to the toxic side effects of the antibody conjugate.

6. Conclusions

This work provides new insight into the molecular determinants underlying BCR silencing in HGBCL-DH-*BCL2*. Through an integrated analysis of immunoglobulin gene rearrangements, IGH class usage, and *CD79B* transcript expression, the study demonstrates that loss of BCR expression in these tumors is not primarily driven by destructive mutations affecting *IGH V* genes or by consistent downregulation of CD79B. Instead, the data point to a model in which the developmental state of the lymphoma precursor cell plays a central role: tumors arising from class-switched B cells frequently lose surface IGH expression, while those retaining IgM expression preserve a functional BCR. In addition, the recurrent detection of multiple light-chain rearrangements in IGH-undetectable tumors suggests that receptor editing may represent an additional mechanism contributing to disruption of BCR assembly. Together, these findings refine our understanding of how aggressive germinal-center–derived lymphomas can evolve independently of canonical BCR signalling pathways and highlight the importance of immunoglobulin gene configuration in shaping the biological heterogeneity of HGBCL-DH-*BCL2*. By clarifying the molecular basis of BCR loss, this work also provides a framework for interpreting variability in response to BCR-targeted therapies and underscores the need to consider BCR expression status when designing therapeutic strategies for these highly aggressive malignancies.

6.1. Limitations of the study

A limitation of this study is the relatively small number of primary cases analysed. Although the findings are consistent and mechanistically coherent, validation in larger cohorts will be necessary to confirm their general applicability. Functional validation of the proposed mechanisms responsible for BCR silencing particularly those related to receptor editing, protein folding, and CD79B turnover, will be required to establish causality.

6.2. Future perspectives

Future work should focus on dissecting the upstream triggers of BCR silencing. One attractive hypothesis is that chronic engagement of autoreactive BCRs may drive progressive receptor desensitization and eventual silencing as an adaptive response to prevent signalling-induced hyperactivation leading to cell death. This hypothesis can be tested through the generation of recombinant antibodies derived from paired IGH and IGL chain V gene sequences cloned from primary lymphoma cass to assess antigen specificity and evaluate their self-reactivity.

Investigations of post-translational regulation of CD79B, including the role of KLHL4 and related pathways, can contribute to understand the mechanisms governing BCR silencing in IGH^{UND} HGBCL-DH-*BCL2*.

7. References

Alcaide, M., Cheung, M., Hillman, J., Rassekh, S.R., Deyell, R.J., Batist, G., Karsan, A., Wyatt, A.W., Johnson, N., Scott, D.W. and Morin, R.D., 2020. Evaluating the quantity, quality and size distribution of cell-free DNA by multiplex droplet digital PCR. *Scientific reports*, *10*(1), p.12564.

Alfarano, A., Indraccolo, S., Circosta, P., Minuzzo, S., Vallario, A., Zamarchi, R., Fregonese, A., Calderazzo, F., Faldella, A., Aragno, M., Camaschella, C., Amadori, A. & Caligaris-Cappio, F., 1999. An alternatively spliced form of *CD79b* gene may account for altered B-cell receptor expression in B-chronic lymphocytic leukemia. *Blood, 93*(7), pp.2327–2335

Amirifar, P., Yazdani, R., Azizi, G., Ranjouri, M.R., Durandy, A., Plebani, A., Lougaris, V., Hammarstrom, L., Aghamohammadi, A. and Abolhassani, H., 2021. Known and potential molecules associated with altered B cell development leading to predominantly antibody deficiencies. *Pediatric Allergy and Immunology*, *32*(8), pp.1601-1615.

Amodio, V., Vitiello, P.P., Bardelli, A. and Germano, G., 2024. DNA repair-dependent immunogenic liabilities in colorectal cancer: opportunities from errors. *British Journal of Cancer*, *131*(10), pp.1576-1590.

Aribi, M., 2020. Introductory chapter: B-Cells. In: *IntechOpen eBooks*. [online] https://doi.org/10.5772/intechopen.90636.

Bagnara, D., Mazzarello, A.N., Ghiotto, F., Colombo, M., Cutrona, G., Fais, F. and Ferrarini, M., 2022. Old and new facts and speculations on the role of the B cell receptor in the origin of chronic lymphocytic leukemia. *International Journal of Molecular Sciences*, *23*(22), p.14249.

Balaji, S., Ahmed, M., Lorence, E., Yan, F., Nomie, K. and Wang, M., 2018. NF-κ B signaling and its relevance to the treatment of mantle cell lymphoma. *Journal of hematology & oncology*, *11*(1), p.83.

Bassing, C.H., Swat, W. and Alt, F.W., 2002. *The mechanism and regulation of chromosomal V(D)J recombination*. [online] *Cell*. Available at: <https://www.cell.com/action/showPdf?pii=S0092-8674%2802%2900675-X> [Accessed 20 March 2026].

Berry, C.T., Liu, X., Myles, A., Nandi, S., Chen, Y.H., Hershberg, U., Brodsky, I.E., Cancro, M.P., Lengner, C.J., May, M.J. and Freedman, B.D., 2020. BCR-induced Ca2+ signals

dynamically tune survival, metabolic reprogramming, and proliferation of naive B cells. *Cell reports*, *31*(2).

Blanco, M., Collazo-Lorduy, A., Yanguas-Casás, N., Calvo, V. and Provencio, M., 2022. Unveiling the role of the tumor microenvironment in the treatment of follicular lymphoma. *Cancers*, *14*(9), p.2158.

Bransteitter, R., Sneeden, J.L., Allen, S., Pham, P. and Goodman, M.F., 2006. First AID (Activation-induced cytidine deaminase) is needed to produce high affinity isotype-switched antibodies. *Journal of Biological Chemistry*, [online] 281(25), pp.16833–16836. https://doi.org/10.1074/jbc.r600006200.

Brian 4th, B.F. and Freedman, T.S., 2021. The Src-family kinase Lyn in immunoreceptor signaling. *Endocrinology*, *162*(10), p.bqab152.

Burger, J.A. and Wiestner, A., 2018. Targeting B cell receptor signalling in cancer: preclinical and clinical advances. *Nature Reviews Cancer*, *18*(3), pp.148-167.

Camus, V., & Tilly, H. (2021). *Polatuzumab vedotin, an anti-CD79b antibody-drug conjugate for the treatment of relapsed/refractory diffuse large B-cell lymphoma*. Future Oncology, 17**(**2), 127–135.

Casola, S., Perucho, L., Tripodo, C., Sindaco, P., Ponzoni, M. and Facchetti, F., 2019. The B-cell receptor in control of tumor B-cell fitness: Biology and clinical relevance. *Immunological reviews*, *288*(1), pp.198-213.

Chaudhuri, J. & Alt, F. W. (2004). Class-switch recombination: interplay of transcription, DNA deamination and DNA repair. *Nature Reviews Immunology*, 4(7), 541–552.

Chen, Z., Miao, C., Zhang, Y., Huang, J., Sun, Y., Chen, J., Sun, J., Shi, W., Wang, X., Wang, R. and Li, Y., 2025. FcRL1, a new B-cell-activating co-receptor. *International Journal of Molecular Sciences*, *26*(13), p.6306.

Chi, X., Li, Y. and Qiu, X., 2020. V (D) J recombination, somatic hypermutation and class switch recombination of immunoglobulins: mechanism and regulation. *Immunology*, *160*(3), pp.233-247.

Choi, J., et al. (2020). *Regulation of B cell receptor-dependent NF-κB signaling by KLHL14 and its impact on BCR subunit stability***.** Proceedings of the National Academy of Sciences USA, 117**(**7), 6092–6102.

Cui, M., Huang, J., Zhang, S., Liu, Q., Liao, Q. and Qiu, X., 2021. Immunoglobulin expression in cancer cells and its critical roles in tumorigenesis. *Frontiers in immunology*, *12*, p.613530.

Damelang, T., Brinkhaus, M., van Osch, T.L., Schuurman, J., Labrijn, A.F., Rispens, T. and Vidarsson, G., 2024. Impact of structural modifications of IgG antibodies on effector functions. *Frontiers in immunology*, *14*, p.1304365.

Degn, S.E. and Tolar, P., 2025. Towards a unifying model for B-cell receptor triggering. *Nature Reviews Immunology*, *25*(2), pp.77-91.

Döring, S., Tscheuschner, G., Flemig, S., Weller, M.G. and Konthur, Z., 2025. Cost-Effective Method for Full-Length Sequencing of Monoclonal Antibodies from Hybridoma Cells. *Antibodies*, *14*(3), p.72.

Efremov, D.G., Turkalj, S. and Laurenti, L., 2020. Mechanisms of B cell receptor activation and responses to B cell receptor inhibitors in B cell malignancies. *Cancers*, *12*(6), p.1396.

Forconi, F., Lanham, S.A. and Chiodin, G., 2022. Biological and clinical insight from analysis of the tumor b-cell receptor structure and function in chronic lymphocytic leukemia. *Cancers*, *14*(3), p.663.

Gehringer, F., Weissinger, S.E., Möller, P., Wirth, T. and Ushmorov, A., 2020. Physiological levels of the PTEN-PI3K-AKT axis activity are required for maintenance of Burkitt lymphoma. *Leukemia*, *34*(3), pp.857-871.

Glass, D.R., Tsai, A.G., Oliveria, J.P., Hartmann, F.J., Kimmey, S.C., Calderon, A.A., Borges, L., Glass, M.C., Wagar, L.E., Davis, M.M. and Bendall, S.C., 2020. An integrated multi-omic single-cell atlas of human B cell identity. *Immunity*, *53*(1), pp.217-232.

Gracie, C.J., Mitchell, R., Johnstone, J.C. and Clarke, A.J., 2025. The unusual metabolism of germinal center B cells. *Trends in Immunology*, [online] 46(5), pp.416–428. https://doi.org/10.1016/j.it.2025.02.015.

Hanscom, T. and McVey, M., 2020. Regulation of error-prone DNA double-strand break repair and its impact on genome evolution. *Cells*, *9*(7), p.1657.

Härzschel, A., Zucchetto, A., Gattei, V. and Hartmann, T.N., 2020. VLA-4 expression and activation in B cell malignancies: functional and clinical aspects. *International Journal of Molecular Sciences*, *21*(6), p.2206.

Hübschmann, D., Kleinheinz, K., Wagener, R., Bernhart, S.H., López, C., Toprak, U.H., Sungalee, S., Ishaque, N., Kretzmer, H., Kreuz, M. and Waszak, S.M., 2021. Mutational mechanisms shaping the coding and noncoding genome of germinal center derived B-cell lymphomas. *Leukemia*, *35*(7), pp.2002-2016.

Huse, K., Bai, B., Hilden, V.I., Bollum, L.K., Våtsveen, T.K., Munthe, L.A., Smeland, E.B., Irish, J.M., Wälchli, S. and Myklebust, J.H., 2022. Mechanism of CD79A and CD79B support for IgM+ B cell fitness through B cell receptor surface expression. *The Journal of Immunology*, *209*(10), pp.2042-2053.

Kapoor, I., Li, Y., Sharma, A., Zhu, H., Bodo, J., Xu, W., Hsi, E.D., Hill, B.T. and Almasan, A., 2019. Resistance to BTK inhibition by ibrutinib can be overcome by preventing FOXO3a nuclear export and PI3K/AKT activation in B-cell lymphoid malignancies. *Cell death & disease*, *10*(12), p.924.

Kotagiri, P., Mescia, F., Rae, W.M., Bergamaschi, L., Tuong, Z.K., Turner, L., Hunter, K., Gerber, P.P., Hosmillo, M., Hess, C. and Clatworthy, M.R., 2022. B cell receptor repertoire kinetics after SARS-CoV-2 infection and vaccination. *Cell reports*, *38*(7).

Lebedin, M. and de la Rosa, K., 2024. Diversification of antibodies: from V (D) J recombination to somatic exon shuffling. *Annual Review of Cell and Developmental Biology*, *40*(1), pp.265-281.

Levy, G., Kicinski, M., Van der Straeten, J., Uyttebroeck, A., Ferster, A., De Moerloose, B., Dresse, M.F., Chantrain, C., Brichard, B. and Bakkus, M., 2022. Immunoglobulin heavy chain high-throughput sequencing in pediatric B-precursor acute lymphoblastic leukemia: is the clonality of the disease at diagnosis related to its prognosis?. *Frontiers in pediatrics*, *10*, p.874771.

Li, J., Yin, W., Jing, Y., Kang, D., Yang, L., Cheng, J., Yu, Z., Peng, Z., Li, X., Wen, Y. and Sun, X., 2019. The coordination between B cell receptor signaling and the actin cytoskeleton during B cell activation. *Frontiers in immunology*, *9*, p.3096.

Li, S., Peng, Y. and Panchenko, A.R., 2022. DNA methylation: Precise modulation of chromatin structure and dynamics. *Current opinion in structural biology*, *75*, p.102430.

Liu, J.C., Zhang, K., Zhang, X., Guan, F., Zeng, H., Kubo, M., Lee, P., Candotti, F., James, L.K., Camara, N.O.S. and Benlagha, K., 2024. Immunoglobulin class-switch recombination: Mechanism, regulation, and related diseases. *MedComm*, *5*(8), p.e662.

Liu, L., Lucas, R.M., Nanson, J.D., Li, Y., Whitfield, J., Curson, J.E., Tuladhar, N., Alexandrov, K., Mobli, M., Sweet, M.J. and Kobe, B., 2022. The transmembrane adapter SCIMP recruits tyrosine kinase Syk to phosphorylate Toll-like receptors to mediate selective inflammatory outputs. *Journal of Biological Chemistry*, *298*(5).

Madrid, D.J., Santhanakrishnan, M., Liu, J., Gibb, D.R., Liu, D., Natarajan, P., Beitler, D., Shi, Z., Mo, C., Tormey, C.A. and Patel, S.R., 2018. Transfused platelets enhance alloimmune responses to transfused KEL-expressing red blood cells in a murine model. *Blood Transfusion*, *17*(5), p.368.

Martinez-Riano, A., Wang, S., Boeing, S., Minoughan, S., Casal, A., Spillane, K.M., Ludewig, B. and Tolar, P., 2023. Long-term retention of antigens in germinal centers is controlled by the spatial organization of the follicular dendritic cell network. *Nature immunology*, *24*(8), pp.1281-1294.

Mazlan, A.H., Muhamad Najib, M.H.A., Hazizul Hassan, M., Mohd Hatta, F.H. and Mohd Yusoff, R., 2024. Effect of DNA template concentration on standard polymerase chain reaction. *International Journal of Pharmaceuticals, Nutraceuticals and Cosmetic Science (IJPNaCS)*, *7*(1), pp.1-11.

Mitiushkina, N.V., Tiurin, V.I., Anuskina, A.A., Bordovskaya, N.A., Nalivalkina, E.A., Terina, D.M., Berkut, M.V., Shestakova, A.D., Syomina, M.V., Kuligina, E.S. and Togo, A.V., 2024. Use of 3′ Rapid Amplification of cDNA Ends (3′ RACE)-Based Targeted RNA Sequencing for Profiling of Druggable Genetic Alterations in Urothelial Carcinomas. *International Journal of Molecular Sciences*, *25*(22), p.12126.

Mlynarczyk, C., Fontán, L. and Melnick, A., 2019. Germinal center-derived lymphomas: The darkest side of humoral immunity. *Immunological reviews*, *288*(1), pp.214-239.

Montesinos-Rongen, M., Brunn, A., Sanchez-Ruiz, M., Küppers, R., Siebert, R. and Deckert, M., 2021. Impact of a faulty germinal center reaction on the pathogenesis of primary diffuse large B cell lymphoma of the central nervous system. *Cancers*, *13*(24), p.6334.

Nielsen, S.C., Yang, F., Jackson, K.J., Hoh, R.A., Röltgen, K., Jean, G.H., Stevens, B.A., Lee, J.Y., Rustagi, A., Rogers, A.J. and Powell, A.E., 2020. Human B cell clonal expansion and convergent antibody responses to SARS-CoV-2. *Cell host & microbe*, *28*(4), pp.516-525.

Ondrisova, L. and Mraz, M., 2020. Genetic and non-genetic mechanisms of resistance to BCR signaling inhibitors in B cell malignancies. *Frontiers in oncology*, *10*, p.591577.

Pal Singh, S., Dammeijer, F. and Hendriks, R.W., 2018. Role of Bruton's tyrosine kinase in B cells and malignancies. *Molecular cancer*, *17*(1), p.57.

Patton, J.T. and Woyach, J.A., 2024, April. Targeting the B cell receptor signaling pathway in chronic lymphocytic leukemia. In *Seminars in Hematology* (Vol. 61, No. 2, pp. 100-108). WB Saunders.

Pethe, A. and Hartmann, T.N., 2025. The cytoskeletal control of B cell receptor and integrin signaling in normal B cells and chronic lymphocytic leukemia. *FEBS letters*, *599*(20), pp.2878-2895.

Pilzecker, B. and Jacobs, H., 2019. Mutating for good: DNA damage responses during somatic hypermutation. *Frontiers in immunology*, *10*, p.438.

Preite, S., Gomez-Rodriguez, J., Cannons, J.L. and Schwartzberg, P.L., 2019. T and B-cell signaling in activated PI3K delta syndrome: From immunodeficiency to autoimmunity. *Immunological Reviews*, *291*(1), pp.154-173.

Profitos-Peleja, N., Santos, J.C., Marin-Niebla, A., Roue, G. and Ribeiro, M.L., 2022. Regulation of B-cell receptor signaling and its therapeutic relevance in aggressive B-cell lymphomas. *Cancers*, *14*(4), p.860.

Rastogi, I., Jeon, D., Moseman, J.E., Muralidhar, A., Potluri, H.K. and McNeel, D.G., 2022. Role of B cells as antigen presenting cells. *Frontiers in immunology*, *13*, p.954936.

Raza, I.G. and Clarke, A.J., 2021. B cell metabolism and autophagy in autoimmunity. *Frontiers in Immunology*, *12*, p.681105.

Seon, B.K., Okazaki, M., Duzen, J., Matsuno, F., Goey, A.K. and Maguire, O., 2024. Identification of unique molecular heterogeneity of human CD79, the signaling component of the human B cell antigen receptor (BCR), and synergistic potentiation of the CD79-targeted therapy of B cell tumors by co-targeting of CD79a and CD79b. *Leukemia research*, *136*, p.107436.

Seon, B.K., Okazaki, M., Duzen, J., Matsuno, F., Goey, A.K. and Maguire, O., 2024. Identification of unique molecular heterogeneity of human CD79, the signalling component of the human B cell antigen receptor (BCR), and synergistic potentiation of the CD79-targeted therapy of B cell tumours by co-targeting of CD79a and CD79b. *Leukemia research*, *136*, p.107436.

Spakman, D., King, G.A., Peterman, E.J. and Wuite, G.J., 2020. Constructing arrays of nucleosome positioning sequences using Gibson Assembly for single-molecule studies. *Scientific Reports*, *10*(1), p.9903.

Takigawa, H., Kitadai, Y., Shimizu, D., Ariyoshi, M., Takasago, T., Tsuboi, A., Tanaka, H., Yamashita, K., Hiyama, Y., Kishida, Y. and Urabe, Y., 2025. Clinical utility of repeated IgH gene rearrangement testing for the diagnosis and surveillance of gastric MALT lymphoma. *Scientific Reports*, *15*(1), p.31657

Thurner, L., Hartmann, S., Neumann, F., Hoth, M., Stilgenbauer, S., Küppers, R., Preuss, K.D. and Bewarder, M., 2020. Role of specific B-cell receptor antigens in lymphomagenesis. *Frontiers in oncology*, *10*, p.604685.

Thurner, L., Hartmann, S., Neumann, F., Hoth, M., Stilgenbauer, S., Küppers, R., Preuss, K.D. and Bewarder, M., 2020. Role of specific B-cell receptor antigens in lymphomagenesis. *Frontiers in oncology*, *10*, p.604685.

Tkachenko, A., Kupcova, K. and Havranek, O., 2023. B-cell receptor signaling and beyond: the role of Igα (CD79a)/Igβ (CD79b) in normal and malignant B cells. *International Journal of Molecular Sciences*, *25*(1), p.10.

Upadhyay, A.A., Kauffman, R.C., Wolabaugh, A.N., Cho, A., Patel, N.B., Reiss, S.M., Havenar-Daughton, C., Dawoud, R.A., Tharp, G.K., Sanz, I. and Pulendran, B., 2018. BALDR: a computational pipeline for paired heavy and light chain immunoglobulin reconstruction in single-cell RNA-seq data. *Genome medicine*, *10*(1), p.20.

Varano, G., Lonardi, S., Sindaco, P., Pietrini, I., Morello, G., Balzarini, P., Vit, F., Neuman, H., Bertolazzi, G., Brambillasca, S., Parr, N. C., Chiarini, M., Bellesi, S., Maiolo, E., Giampaolo, S., Mainoldi, F., Selvarasa, V., Arima, H., Pellegrini, V., … Casola, S. (2025). *B-cell receptor silencing reveals the origin and dependencies of high-grade B-cell lymphomas with MYC and BCL2 rearrangements*. Blood Cancer Discovery**, 6**(4), 364–393.

van Bladel, D.A., van den Brand, M., Rijntjes, J., Naga, S.P., Haacke, D.L., Luijks, J.A., Hebeda, K.M., van Krieken, J.H.J., Groenen, P.J. and Scheijen, B., 2022. Clonality assessment and detection of clonal diversity in classic Hodgkin lymphoma by next-generation sequencing of immunoglobulin gene rearrangements. *Modern Pathology*, *35*(6), pp.757-766.

Vázquez Bernat, N., et al., 2019. High-quality library preparation for NGS-based immunoglobulin germline gene inference and repertoire expression analysis. *Frontiers in Immunology*, 10:660.

Wang, J.Q., et al., 2019. A novel high-grade B-cell lymphoma cell line (COH-THL1) derived from a patient with MYC and BCL2 double-hit lymphoma. *Leukemia Research*, 81, pp.1–9

Wen, Y., Jing, Y., Yang, L., Kang, D., Jiang, P., Li, N., Cheng, J., Li, J., Li, X., Peng, Z. and Sun, X., 2019. The regulators of BCR signaling during B cell activation. *Blood Science*, *1*(02), pp.119-129.

Weniger, M.A., Seifert, M. and Küppers, R., 2024. B cell differentiation and the origin and pathogenesis of human B cell lymphomas. *Lymphoma: Methods and Protocols*, pp.1-30.

Winkler, T.H. and Mårtensson, I.L., 2018. The role of the pre-B cell receptor in B cell development, repertoire selection, and tolerance. *Frontiers in immunology*, *9*, p.2423.

Wong, J.B., Hewitt, S.L., Heltemes-Harris, L.M., Mandal, M., Johnson, K., Rajewsky, K., Koralov, S.B., Clark, M.R., Farrar, M.A. and Skok, J.A., 2019. B-1a cells acquire their unique characteristics by bypassing the pre-BCR selection stage. *Nature communications*, *10*(1), p.4768.

Xu, Y., Zhou, H., Post, G., Zan, H. and Casali, P., 2022. Rad52 mediates class-switch DNA recombination to IgD. *Nature Communications*, *13*(1), p.980.

Young, C. and Brink, R., 2021. The unique biology of germinal center B cells. *Immunity*, *54*(8), pp.1652-1664.

Young, R.M., Phelan, J.D., Wilson, W.H. and Staudt, L.M., 2019. Pathogenic B-cell receptor signaling in lymphoid malignancies: new insights to improve treatment. *Immunological reviews*, *291*(1), pp.190-213.

Yu, K. and Lieber, M.R., 2019. Current insights into the mechanism of mammalian immunoglobulin class switch recombination. *Critical reviews in biochemistry and molecular biology*, *54*(4), pp.333-351.

Yu, L., Yu, T.T. and Young, K.H., 2019. Cross-talk between Myc and p53 in B-cell lymphomas. *Chronic diseases and translational medicine*, *5*(03), pp.139-154.

Acknowledgement

First and foremost, my deepest gratitude goes to my supervisor, Dr. Stefano Casola. His guidance, advice, and unwavering support have been instrumental throughout my journey. His patient explanations of the intricate details of the topic and his relentless commitment to helping me comprehend the underlying biology of the experiments have been invaluable. I am truly fortunate to have had his mentorship.

I extend heartfelt thanks to the members of our research group, especially Gabrielle Varano and Federico Mainoldi. Their collaborative spirit, assistance in the laboratory, and continuous supervision have been crucial to the successful execution of my wet lab work. Their readiness to offer guidance and correct my mistakes has been a constant source of learning and growth. Their physical and intellectual support has been truly appreciated.

A special acknowledgment goes to the IFOM campus for providing me with the opportunity to undertake my master's thesis. The conducive research environment and resources available were essential in facilitating my academic pursuits.

I wish to express sincere gratitude to Professor Federico Forneris, who graciously accepted the role of my internal supervisor and offered me my initial exposure to the laboratory. My gratitude also extends to Marco Santagostino, the coordinator, for his diligent efforts in managing thesis-related matters and for allowing me the privilege to conduct my research beyond the University of Pavia.

My journey would not have been possible without the unwavering support of my husband, Sivacegaram Anojan. His encouragement and financial support since our arrival as students from Sri Lanka have been my rock. His belief in my potential and his commitment to helping me achieve my goals have been a driving force behind my accomplishments.

I am grateful to my family for their constant encouragement and unwavering belief in me. Their faith has been a guiding light, propelling me forward on the right path.

Lastly, I extend my appreciation to all my friends and relatives for their encouragement, support, and understanding throughout my academic pursuit. Thank you all for being an integral part of my journey and for contributing to my achievements.